Mon. Not. R. Astron. Soc. **268,** 79–102 (1994)

Anisotropic mergers at high redshifts: the formation of cD galaxies and powerful radio sources

Michael J. West
Sterrewacht Leiden, Postbus 9513, 2300 RA Leiden, The Netherlands

Accepted 1993 November 29. Received 1993 October 26; in original form 1993 June 28

ABSTRACT

A new dynamical model for the formation of dominant cluster galaxies and powerful radio sources at high redshifts is proposed. In this model, powerful high-redshift radio galaxies are assumed to represent an early stage in the formation of massive cD galaxies in the centres of rich clusters, corresponding to an epoch when these galaxies were being built via mergers of smaller gas-rich protogalactic units. It is argued that in many cosmogonies such mergers will not occur haphazardly, but rather will proceed in a coherent or 'organized' manner along preferred axes which are related to large-scale anisotropies in the primordial density field. As a consequence of this anisotropic formation process, these galaxies are quite *prolate* in shape and have a built-in 'memory' of their surroundings, even at high redshifts. Such a formation scenario can account quite naturally for the observed shapes and kinematics of cD galaxies today, as well as their tendency to be aligned with the major axis of their parent cluster and the galaxy distribution on much larger scales.

Frequent mergers during this early formation phase are likely to provide an abundant source of gas-rich material. Cold gas falling into the prolate potential well of these burgeoning galaxies will quickly settle into a disc whose angular momentum vector is aligned with the *major* axis of the (proto)galaxy mass distribution. Angular momentum loss during this settling process results in an inward flow of gas towards the centre of the young galaxy, which provides a plentiful source of material for both the creation and feeding of a central black hole. It is argued that under these circumstances the black hole spin axis will align with the angular momentum vector of the fuelling accretion disc, and hence its orientation will ultimately be determined by the intrinsic shape and orientation of the host galaxy. In the standard 'twin-exhaust' model for active galactic nuclei, the radio jets are expected to emanate along the black hole spin axis, and thus will tend to align with the major axis of the mass distribution in these prolate protogalaxies. It is for this reason that the extended optical and infrared components of powerful high-z radio galaxies are often closely aligned with the radio axis.

The model proposed here implies a truly remarkable coherence of structures from the central engines in active galactic nuclei to the large-scale structure of the Universe. Several low-redshift analogues to powerful high-redshift radio galaxies are discussed and shown to exhibit properties that suggest that they may indeed have formed in the manner described here. A number of testable predictions of this model are also made.

Key words: galaxies: active – galaxies: elliptical and lenticular, cD – galaxies: formation – galaxies: interactions – galaxies: jets – radio continuum: galaxies.

1 INTRODUCTION: A TALE OF TWO ALIGNMENT EFFECTS

1.1 High-redshift radio galaxies

Ever since Baade & Minkowski (1954) first identified the powerful radio source Cygnus A with a giant elliptical galaxy at redshift $z = 0.056$, radio galaxies have ranked among the most extraordinary and enigmatic objects in the sky. Because they can be observed over a wide range of redshifts, and hence epochs, radio galaxies may well turn out to be a sort of cosmological Rosetta Stone which will enable astronomers to decipher important clues about galaxy formation and the energetics of active galactic nuclei.

Considerable insight has been gained in recent years into the nature of powerful radio galaxies at high redshifts (see McCarthy 1993 for a review). It is now clear that many of these galaxies have rather complex morphologies compared to their low-redshift counterparts. CCD observations have revealed that the majority of 3C radio galaxies at $z > 1$ are quite elongated and clumpy in appearance, often extending 20–30 h^{-1} kpc or more[1] (e.g. Djorgovski et al. 1987; McCarthy et al. 1987; Chambers, Miley & Joyce 1988; Le Fèvre, Hammer & Jones 1988; Hammer & Le Fèvre 1990). Under good seeing conditions many of these galaxies are resolved into multiple components which are often distributed in a quasi-linear configuration. Recent *Hubble Space Telescope* (*HST*) observations of the most distant known radio galaxy, 4C 41.17 at $z = 3.8$, have shown this galaxy to be extremely clumpy and elongated even on sub-kiloparsec scales (Miley et al. 1992). Miley (1992) has also commented on the high incidence of double structures among distant radio galaxies.

Yet perhaps the most intriguing property of these high-z radio galaxies was the discovery that their extended optical (restframe ultraviolet) structure is often closely aligned with the radio source axis (e.g. Chambers, Miley & van Breugel 1987; McCarthy et al. 1987; Le Fèvre & Hammer 1988). This phenomenon is illustrated in Fig. 1, which shows a histogram of the difference between the radio and optical major-axis orientations for a sample of more than 40 distant 3C radio galaxies (compiled from a number of published studies; see Fig. 1). The discovery of this radio–optical alignment effect was quickly followed by evidence that the infrared (restframe optical) component of many of these galaxies also exhibits a similar, although weaker, alignment tendency (Chambers et al. 1988; Eales & Rawlings 1990; Eisenhardt & Chokshi 1990; Rigler et al. 1992; Dunlop & Peacock 1993). The alignment effect shows a strong evolution with redshift, being ubiquitous at $z \gtrsim 1$ but absent at low redshifts (see e.g. McCarthy & van Breugel 1989). Dunlop & Peacock (1993) have recently suggested that this may reflect a dependence on radio luminosity rather than epoch.

The origin of the radio–optical–infrared alignments in high-redshift radio galaxies is unclear at present, and has been a subject of considerable debate. Among the explanations that have been proposed to date are

(i) vigorous star formation triggered by the passage of the radio jets through a surrounding gaseous medium (Chambers et al. 1987; McCarthy et al. 1987; De Young 1989; Rees 1989; Daly 1990);

(ii) scattered light from an obscured quasar nucleus (di Serego Alighieri et al. 1989; Eales & Rawlings 1990; Fabian 1989);

(iii) gravitational lensing (Le Fèvre, Hammer & Jones 1988; Hammer & Le Fèvre 1990);

(iv) non-thermal mechanisms such as optical synchrotron radiation, or inverse Compton scattering of microwave background photons by relativistic electrons associated with the radio jet (Chambers et al. 1988; Daly 1992);

(v) mergers associated with the formation of massive galaxies (Djorgovski et al. 1987; West 1991a,b, 1993a), and

(vi) observational selection effects favouring aligned over unaligned sources (Djorgovski 1987; Eales 1992).

While these proposed mechanisms can explain the alignment effect with varying degrees of success, none has proven entirely satisfactory at accounting for the full range of high-z radio galaxy properties (see Chambers & Miley 1990; Daly 1992; Dunlop & Peacock 1993; McCarthy 1993 for critical reviews). For example, models that invoke jet-induced star formation to explain the alignment effect require uncomfortably high birthrates of massive stars which may be difficult to reconcile with their observed spectral energy distributions (e.g. Rocca-Volmerange & Guiderdoni 1990). Furthermore, direct observational evidence that radio jets can stimulate the sort of copious star formation required to explain the alignment effect is markedly scant – with the exception of one or two anecdotal cases such as Minkowski's object (van Breugel et al. 1985), powerful nearby radio galaxies do not appear to stimulate abundant star formation, despite their frequent location in gas-rich environments. Scattering (whether by dust or electrons) models also face a number of difficulties, and it seems likely that only a small fraction of the aligned light can be attributed to this origin (e.g. Eales & Rawlings 1990).

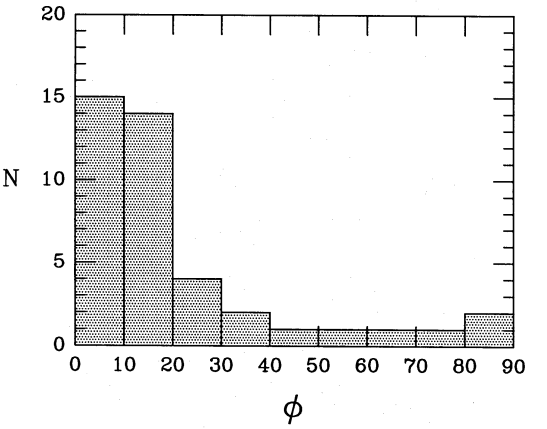

Figure 1. The alignment effect in powerful 3C radio galaxies at high redshifts ($z \gtrsim 0.6$). Shown here is the frequency distribution of the difference, ϕ, between the position angles of the optical major axis and the radio axis. Data were combined from studies by McCarthy et al. (1987), Le Fèvre & Hammer (1988). Le Fèvre et al. (1988), Hammer & Le Fèvre (1990), Rigler et al. (1992), and Dunlop & Peacock (1993). The alignment tendency is significant at greater than the 99.9 per cent confidence level.

[1]Here and throughout, $H_0 \equiv 100\ h$ km s^{-1} Mpc^{-1} and $q_0 = 0.5$ will be adopted.

The possibility that this alignment effect might actually be what the most naive interpretation of these observations would suggest – a correlation between the principal axis of the mass distribution of the host galaxy and the radio jets – has been repeatedly rejected in the literature. Spinrad (1989), for example, argued that 'There would seem to be no obvious reason why accumulation of dark or luminous subunits would occur along the radio axis; probably the procedure is reversed and the radio source somehow channels the axis of new star formation.' Chambers & Miley (1990) likewise dismissed the possibility that the radio jet orientation might be sensitive to the galaxy mass distribution as 'a difficult proposition to believe.' Yet it is precisely this possibility that will be considered in later sections of this paper.

1.2 Brightest cluster galaxies at low redshifts

There is a *second* alignment effect, seemingly unrelated to the first, which involves cD and brightest cluster galaxies (BCGs) at low redshifts.[2]

It is well established that BCGs in Abell clusters show a strong propensity to be aligned with the major axis of their parent cluster (Sastry 1968; Carter & Metcalfe 1980; Binggeli 1982; Struble & Peebles 1985; West 1989; van Kampen & Rhee 1990; Porter, Schneider & Hoessel 1991). Furthermore, there is mounting evidence that the orientations of BCGs and their parent clusters are correlated with the surrounding matter distribution on much larger scales (see West 1994 for a review). For example, numerous studies have shown that the major axes of Abell clusters and their BCGs exhibit a conspicuous tendency to 'point' towards other neighbouring clusters over separations of up to several tens of Mpc (e.g. Binggeli 1982; Rhee & Katgert 1987; West 1989; Lambas et al. 1990; Plionis, Valdarnini & Jing 1992; Rhee, van Haarlem & Katgert 1992; West & Schombert, in preparation). Similarly, Argyres et al. (1986) and Lambas, Groth & Peebles (1988) found that galaxy counts out to distances of $\sim 15\ h^{-1}$ Mpc from the centres of Abell clusters are systematically higher along the direction defined by the major axis of the BCG.

Proof that there exists a fundamental connection between the structure of BCGs and the surrounding matter distribution on much larger scales is provided by Fig. 2. Here the projected major-axis orientations of the *innermost* ($r \lesssim 2\ h^{-1}$ kpc) regions of a sample of 147 BCGs in Abell clusters have been compared with the distribution of all neighbouring Abell clusters within a distance of $10\ h^{-1}$ Mpc. The BCG major-axis position angles were taken from data published by Porter et al. (1991), and Abell cluster redshifts were taken from the recent compilation by Peacock & West (1992). The difference between the position angle of the BCG major axis and the position angle between the galaxy and a neighbouring cluster defines a BCG alignment angle, θ, whose frequency distribution is shown in Fig. 2.

What Fig. 2 shows is remarkable evidence that the orientations of even the innermost $\sim 2\ h^{-1}$ kpc regions of

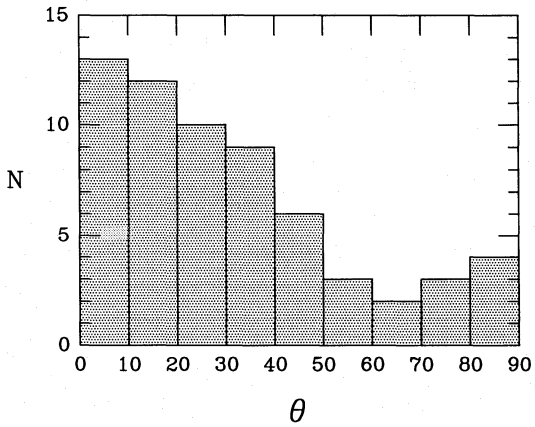

Figure 2. Alignment of the innermost regions of a sample of 147 BCGs with their large-scale environs. Here θ is the acute angle between the projected BCG major axis at a radius of $\sim 2\ h^{-1}$ kpc (taken from Porter et al. 1991) and the great circle between the BCG and another neighbouring Abell cluster within $10\ h^{-1}$ Mpc ($\theta = 0°$ if the BCG major axis points exactly at the neighbouring cluster). The significance of the alignment effect exceeds the 99.9 per cent confidence level.

BCGs are strongly correlated with the surrounding distribution of matter on scales of at least $10\ h^{-1}$ Mpc. *Information about the distribution of neighbouring rich clusters has somehow been communicated to the very cores of these BCGs.* Although weaker than the alignment effect seen in Fig. 1, this tendency for the BCG major axes to 'point' towards neighbouring Abell clusters is nevertheless highly significant; various statistical tests indicate a probability of much less than 1 per cent that the distribution seen in Fig. 2 is consistent with random BCG orientations. A similar alignment tendency is seen if the BCG major-axis orientations at larger radii are used instead.

It is important to note that *only BCGs exhibit such an alignment effect*; other galaxies show no evidence for preferred orientations (Struble 1990; van Kampen & Rhee 1990; Trevese, Cirimele & Flin 1992). This strongly suggests that BCGs are the product of a 'special' formation history, and that their properties are closely linked to the formation of structures on larger scales. Indeed, it has often been suggested that the BCGs are a distinct class of galaxies, rather than simply the extreme end of a continuum of elliptical galaxy morphologies (see Dressler 1984, Tremaine 1990 and Schombert 1992 for reviews from various perspectives). This claim is based on such observed properties as

(1) their enormous masses and luminosities, $M_{\rm tot} \gtrsim 10^{12}$ $M_\odot$ and $L_{\rm tot} \gtrsim 10^{11}$ $L_\odot$;

(2) their distinctive photometric and kinematic traits (e.g. Schombert 1988; Oegerle & Hoessel 1991; Porter et al. 1991);

(3) the remarkably small dispersion in their absolute magnitudes (Sandage 1976; Hoessel 1980; Bhavsar 1989);

(4) the fact that they are generally found only in very dense environments, usually the centres of rich clusters (Beers & Geller 1983);

[2]The terms 'cD' and 'BCG' will be used interchangeably throughout this paper to denote first-ranked elliptical galaxies in rich clusters which are very much dominant over any other cluster members. Strictly speaking, however, not all BCGs are cD galaxies.

(5) the high frequency of secondary or multiple nuclei in BCGs (Hoessel & Schneider 1985; Lauer 1988);

(6) their apparent overabundance of globular clusters (e.g. van den Bergh 1983; Harris 1991; West 1993b);

(7) their highly elongated shapes, which appear to be significantly flatter and more prolate than those of other cluster ellipticals (Leir & van den Bergh 1977; Porter et al. 1991; Ryden, Lauer & Postman 1993), and

(8) their aforementioned alignment tendency.

Two opposing schools of thought regarding the origin of BCGs have emerged over the years. According to one view, cDs started out as 'normal' elliptical galaxies which, because of their fortuitous location at the dynamical centres of rich clusters, grew by slow accretion of material stripped from other cluster galaxies and/or by galactic cannibalism (see Tremaine 1990 for a review). In this picture, the observed alignment of the outer isophotes of BCGs with their parent clusters arises because the accreted halo material presumably reflects the characteristic shape and orientation of the cluster gravitational potential. Most theoretical work to date has focused on this possibility of 'late' (i.e. post-cluster-collapse) cD formation.

There are, however, a number of problems with such a model of BCG formation. First, there is the well-known difficulty of forming giant $\sim 10^{12}$-$M_{\odot}$ galaxies in a Hubble time based on the estimated merger and accretion rate in present-day clusters (see e.g. Merritt 1985; Tremaine 1990). Secondly, the small dispersion in BCG luminosities would seem to require that the growth of these galaxies by cannibalism and accretion was incredibly 'self-regulating' in a wide range of cluster environments. Thirdly, it is difficult to understand in such a model why the very innermost $\sim 2\ h^{-1}$ kpc regions of BCGs should be aligned with their surroundings as in Fig. 2; if BCGs were simply 'normal' elliptical galaxies embedded in an accreted envelope, then like other ellipticals their cores should presumably have random orientations.

The alternative possibility is that BCGs were somehow special *ab initio*, their unique properties having been determined at the time of their birth. Sandage (1976) and Tremaine & Richstone (1977) argued that the narrow range of BCG luminosities indicates that they must have been formed by some 'special process' at early epochs. Van den Bergh (1983) made the interesting suggestion that BCGs might be 'kernels' around which rich clusters formed, speculating that 'the central galaxies in rich clusters were already very special at an early stage in the evolution of their parent clusters.' Yet this possibility that BCGs might somehow have been 'born' special has been little explored to date, perhaps not surprisingly since any such model inevitably involves rather uncertain and speculative physics about the cosmological initial conditions. To explain the alignment effect seen in Fig. 2, for example, would at first glance seem to require something of a 'cosmic conspiracy' whereby the dense inner cores of BCGs, which presumably collapsed well before any clusters or superclusters, somehow 'knew' from the very earliest epochs to align their major axes with the *eventual* distribution of matter on much larger scales. This would require a remarkable coherence of the primordial density field over a wide range of scales.

In this paper a new dynamical model is proposed to explain the different alignment effects seen in Figs 1 and 2. Its basic premise is that powerful radio galaxies at high redshifts are the precursors of the brightest cluster galaxies seen today, and that these galaxies carry the imprint of a rather unique formation history which is reflected in their observed morphologies. The principal conclusion is that the two alignment effects – the radio–optical–infrared alignments of powerful high-z radio galaxies and the alignments of BCGs with their surroundings at low redshifts – are in fact *related* phenomena whose origin can be ascribed to a galaxy formation process characterized by highly *anisotropic mergers*.

2 THE FORMATION OF PROTO-BCGs AT HIGH REDSHIFTS

In most currently popular models for the evolution of structure in the Universe, galaxy formation is envisaged as proceeding in a hierarchical manner, with small subgalactic units merging to produce progressively larger systems. In the standard cold dark matter (CDM) model, for example, galaxy formation is expected to be a fairly recent occurrence, with the majority of galaxies having been assembled at redshifts $z \simeq 1$–3 (e.g. Blumenthal et al. 1984; Frenk et al. 1988; Carlberg & Couchman 1988). That this epoch coincides with the observed peak in quasar and radio galaxy activity suggests an important causal relation between mergers and active galactic nuclei (Efstathiou & Rees 1988; Carlberg 1990; Haehnelt & Rees 1993). It is important to emphasize, however, that CDM is merely one in a broad class of possible hierarchical models whose behaviours are qualitatively similar; the idea that many or most galaxies might have formed by mergers of smaller systems has been around for quite some time (Peebles & Dicke 1968; Toomre 1977).

An important consideration, which has not received much attention to date, is that the mergers that produce massive galaxies at high redshifts are not likely to occur haphazardly. Instead, it is the author's contention that such mergers will generally proceed in a coherent or 'organized' manner along preferred axes which reflect large-scale anisotropies in the surrounding linear density field. *In particular, massive BCGs which form at the centres of nascent protoclusters are likely to be built by a process of predominantly head-on (i.e. low angular momentum) mergers of material shepherded along developing large-scale filamentary features in the matter distribution.* Galaxies formed in such a way will have a 'memory' of their surroundings built into them. These points are elaborated on below.

2.1 BGCs and rich clusters as peaks in the primordial density field

It is widely believed that structures from subgalactic to supercluster scales grew via the gravitational instability of small inhomogeneities which were present in the primordial matter distribution. The first objects to form would have been those that had the largest initial densities (since in general $t_{\rm form} \propto \rho^{-1/2}$), and hence the sequence of formation of structure is uniquely determined by the amplitude of fluctuations on different scales. This is conveniently described in terms of the power spectrum, $P(k)$, defined by

$$P(k) \equiv |\delta_k|^2, \qquad (1)$$

where δ_k denotes the Fourier components of the dimensionless density fluctuation field,

$$\delta \equiv \frac{\rho - \overline{\rho}}{\overline{\rho}}, \tag{2}$$

and k is the spatial frequency of each mode. The primordial power spectrum is generally assumed to have been a monotonically decreasing function of scale, which leads to a hierarchical formation of structure.

A common additional assumption, motivated both by inflationary models and by more general considerations, is that the primordial density field was a Gaussian random process, i.e. on each mass scale the probability distribution of overdensities δ obeys Gaussian statistics. An impressive body of theoretical work has elucidated many of the properties of Gaussian random fields and their implications for structure formation (e.g. Doroshkevich 1970; Blumenthal et al. 1984; Kaiser 1984; Peacock & Heavens 1985; Bardeen et al. 1986). In particular, considerable attention has focused on the possibility that cosmic structures such as galaxies and galaxy clusters might have formed preferentially at the sites of local *maxima* or *peaks* in the density field. Kaiser (1984), for example, argued that because rich Abell clusters are the most massive systems to have collapsed by today it seems likely that they formed from relatively rare $\gtrsim 3\sigma$ fluctuations. He showed that this could account for the stronger clustering of Abell clusters compared to galaxies, since rare high-σ peaks in Gaussian random fields have a statistically enhanced clustering tendency relative to the underlying mass distribution.

Similarly, it has been widely suggested that galaxy formation might have been 'biased' in the sense that bright galaxies formed preferentially at the sites of high peaks (e.g. Davis et al. 1985; Bardeen et al. 1986). A number of authors have further speculated that galaxy type might be related to peak height, with early-type galaxies forming from the highest $\gtrsim 3\sigma$ peaks while late-type galaxies might be associated with more moderate ~ 1–2σ fluctuations (e.g. Blumenthal et al. 1984; Dekel & Silk 1986). If normal bright elliptical galaxies did indeed originate from rare density fluctuations, then massive BCGs located at the centres of rich clusters must surely have formed from the rarest of the rare.

2.2 Correlations between cluster and supercluster scales

One of the most interesting properties of Gaussian random fields is that for a wide range of cosmological initial conditions some amount of 'cross-talk' is expected to occur between density fluctuations on different scales. A measure of the cross-talk between two different mass scales M_a and M_b is given by the correlation coefficient γ, defined as

$$\gamma \equiv \frac{\sigma_{ab}^2}{\sigma_a \sigma_b}, \tag{3}$$

where σ_{ab}^2, σ_a^2 and σ_b^2 denote the variance of the density field smoothed on a scale R with some filter $W(kR)$:

$$\sigma_a^2 = \int P(k)\, W^2(kR_a)\, \mathrm{d}^3 k, \tag{4}$$

$$\sigma_b^2 = \int P(k)\, W^2(kR_b)\, \mathrm{d}^3 k, \tag{5}$$

$$\sigma_{ab}^2 = \int P(k)\, W(kR_a)\, W(kR_b)\, \mathrm{d}^3 k. \tag{6}$$

Assuming a Gaussian filter function and an Einstein–de Sitter ($\Omega = 1$) universe, the mass contained within a sphere of radius R is

$$M = (2\pi)^{3/2} R^3 \overline{\rho} = 4.37 \times 10^{12} R^3\ h^{-1}\ \mathrm{M}_\odot. \tag{7}$$

Fig. 3 shows the expected correlations between cluster and large-scale fluctuations for various scale-free power spectra of the form

$$P(k) \propto k^n, \tag{8}$$

where $\gamma = 1$ by definition on a cluster scale of $10^{15}\ \mathrm{M}_\odot$ ($\gamma = 0$ if there is no correlation between the different mass scales). It is evident from Fig. 3 that significant correlations are expected between cluster and supercluster scales, particularly for flatter power spectra (i.e. more negative values of n). These correlations become even stronger for high-σ peaks, and can be further enhanced by non-linear coupling of Fourier modes which transfer power from large to small scales (Little, Weinberg & Park 1991).

There now exists a sizeable body of observational evidence that the large-scale galaxy distribution is characterized by the presence of strikingly coherent filamentary and sheetlike[3] structures extending 50–100 h^{-1} Mpc or

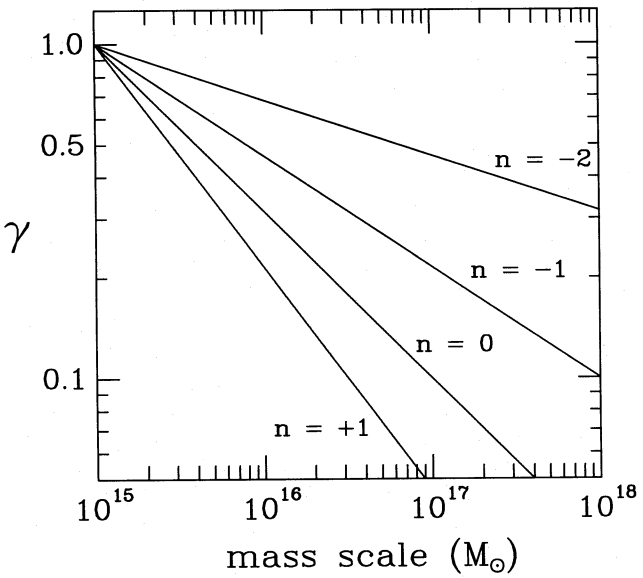

Figure 3. Correlations between cluster and large-scale perturbations. The correlation coefficient γ is defined by equation (3). A cluster mass of $10^{15}\ \mathrm{M}_\odot$ has been assumed, with $\gamma = 1$ by definition on that scale. This figure shows that significant correlations are expected between cluster and supercluster scales, especially for flatter power spectra (i.e. for more negative values of n).

[3]As an operative definition, 'filaments' will be taken here to mean quasi-linear mass concentrations in which one of the three principal axes is very much longer than the others ($l_1 \gg l_2 \sim l_3$), while 'sheets' correspond to quasi-planar structures ($l_1 \sim l_2 \gg l_3$).

more in size (e.g. de Lapparent, Geller & Huchra 1986; Haynes & Giovanelli 1986; Bhavsar & Ling 1988; Geller & Huchra 1989). One of the most interesting, and somewhat surprising, results to emerge from the past decade of cosmological *N*-body simulations has been the realization that the development of a network of interconnected filamentary structures is a rather generic feature of many cosmogonic models. Such structures are naturally expected to arise in 'pancake' models (e.g. hot dark matter) in which the spectrum of density fluctuations possesses a coherence length due to the damping of small-scale perturbations below some critical wavelength (Zeldovich 1970). More unexpected, however, was the discovery that filamentary features also occur in many *hierarchical* clustering models such as CDM and scale-free power spectra with no built-in coherence length (Bond 1986, 1987; White et al. 1987; Efstathiou et al. 1988; Melott & Shandarin 1989; Nusser & Dekel 1990; Weinberg & Gunn 1990; West, Villumsen & Dekel 1991; Kofman et al. 1992). This body of theoretical and numerical work indicates that *any* sufficiently flat spectrum of density fluctuations will lead to the formation of large-scale filamentary structures. Specifically, if the initial power spectrum had the scale-free form $P(k) \propto k^n$, then the criterion for the development of filamentary features appears to be $n \lesssim -1$, with $n \approx -1$ marking the critical transition between cosmogonies driven primarily by the formation of a hierarchy of roughly spherical clumps and those characterized by the emergence of large-scale anisotropic features. Flatter power spectra lead to a more pronounced filamentary appearance.

This behaviour is illustrated in Fig. 4, which shows a typical *N*-body simulation of the evolving mass distribution in a cold dark matter universe (taken from West et al. 1991). The predicted shape of the CDM fluctuation spectrum varies from $P(k) \propto k^{-3} \sim k^{-2}$ on subgalactic and galactic scales to $P(k) \propto k^{-1} \sim k^0$ on the scales of rich clusters and superclusters (Blumenthal et al. 1984; Bond & Efstathiou 1984). Consequently, one would expect a CDM-dominated universe to be characterized by a filamentary texture over a wide range of scales, even though the clustering process is decidedly hierarchical in nature. This leads to concurrent evolutionary effects: the coherent collapse of large-scale perturbations to produce sheets and filaments, the development of small-scale clumps within these structures, and the streaming of material along the filaments towards peaks and nodes where adjacent filaments intersect. Such peaks are the most natural sites for the formation of rich galaxy clusters. Anisotropic structures of various sizes and shapes begin to appear quite early in these simulations, and, as Fig. 4 shows, rich clusters and a large-scale filamentary pattern are easily recognizable even at high redshifts.

Recent observational work (Peacock 1991; Peacock & West 1992; Vogeley et al. 1992; Einasto et al. 1993) has provided the first *direct* determination of the form of the primordial density fluctuation spectrum on scales ~ 10–$100\ h^{-1}$ Mpc; these studies all indicate a power spectrum index $n \approx -1.5 \pm 0.5$ on those scales. A variety of arguments also suggest that a power spectrum index $n \approx -2$ is most consistent with observed galaxy properties (Faber 1982; Blumenthal et al. 1984; White & Frenk 1991). Hence, if *N*-body results serve as a guide, large-scale filamentary structures are likely to be a common feature in the Universe.

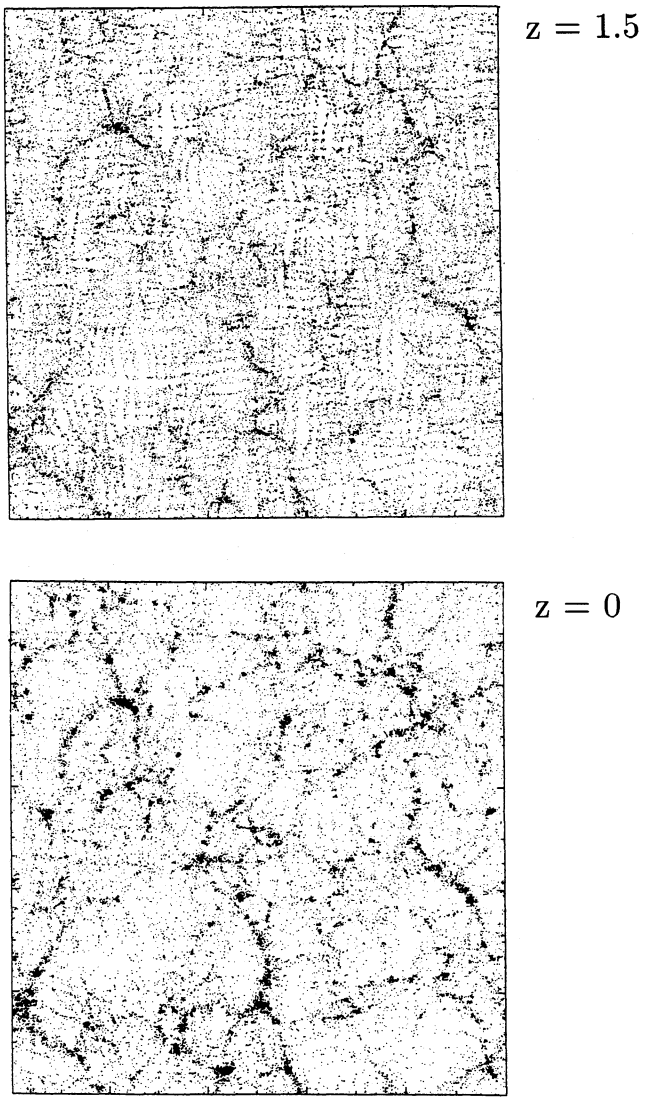

Figure 4. An illustration of the formation of rich clusters and large-scale filamentary features in a typical *N*-body simulation of a CDM universe (taken from West, Villumsen & Dekel 1991). Shown here is a $10\ h^{-1}$ Mpc thick slice through a simulated cube which is $100\ h^{-1}$ Mpc on a side. Note how quickly clusters and filamentary features begin to develop, being quite prominent even at high redshifts.

Furthermore, because of the flatness of the primordial power spectrum one would expect quite strong correlations between cluster and supercluster scales (Fig. 3).

The formation of rich clusters of galaxies, in particular their shapes and orientations, is therefore likely to have been strongly influenced by the statistical properties of the large-scale primordial density field. Bond (1986, 1987) has demonstrated that Gaussian cross-talk can produce quite large anisotropies in the fields around clusters, one consequence of which is that clusters will tend to be born aligned with their surroundings on scales of tens of Mpc (see also West, Dekel & Oemler 1989; West et al. 1991). This presumably is the origin of the alignments of neighbouring clusters discovered by Binggeli (1982).

2.3 BCG formation via anisotropic mergers

The centre of a rich protocluster is certainly a special location; it is here that the deformation tensor of the local density field is greatest, and consequently material flowing along developing filamentary features will accumulate in these deep potential wells. In a sense, the protocluster centre can be likened to a gravitational 'focal point' where infalling material converges. These peaks are natural sites for the genesis of BCGs.

Because of the cross-talk that occurs between cluster and supercluster scales, the flow of material into these high-density regions will be highly anisotropic. As Bardeen et al. (1986) concluded from their seminal study of the statistics of Gaussian random fields, 'The flows are definitely not spherically symmetric into the peak, especially when later accretion from pancaked regions occurs.' *N*-body simulations support these claims: for example, Melott & Shandarin's (1989) high-resolution simulations showed that the development of coherent filamentary features leads to a formation sequence whereby 'the first clumps acquire mass by nonspherical accretion from dense bridges connecting the clumps.' Hence any galaxy that forms at the protocluster centre is likely to experience a quite different formation history from those of other galaxies in more 'typical' environments. *Specifically, massive galaxies destined to become BCGs are formed by a process of agglomeration of smaller clumps which infall anisotropically along preferred axes whose orientations are related to the statistical properties of the large-scale density field.*

How does this sort of anisotropic merger history described above affect the structure of these galaxies? Numerical simulations have shown that in head-on collisions of galaxies the merger remnant is invariably quite *prolate* in shape, with its major axis oriented along the original separation vector between the two pre-merger objects (White 1978, 1979; Villumsen 1982, 1983). High-angular-momentum mergers, on the other hand, tend to produce oblate remnants. *Hence, because they are built up anisotropically by low-angular-momentum mergers along preferred axes, the structures and orientations of these BCGs are closely linked to their surroundings, reflecting the large-scale filamentary pattern of superclustering.* Clusters that form within filaments will be fed in a single preferred direction. Clusters that form at the nodes where different filaments intersect may be built up by material infalling in several directions, but the 'dominant' local filamentary feature is likely to exert the most profound influence on the final cluster/BCG orientation.

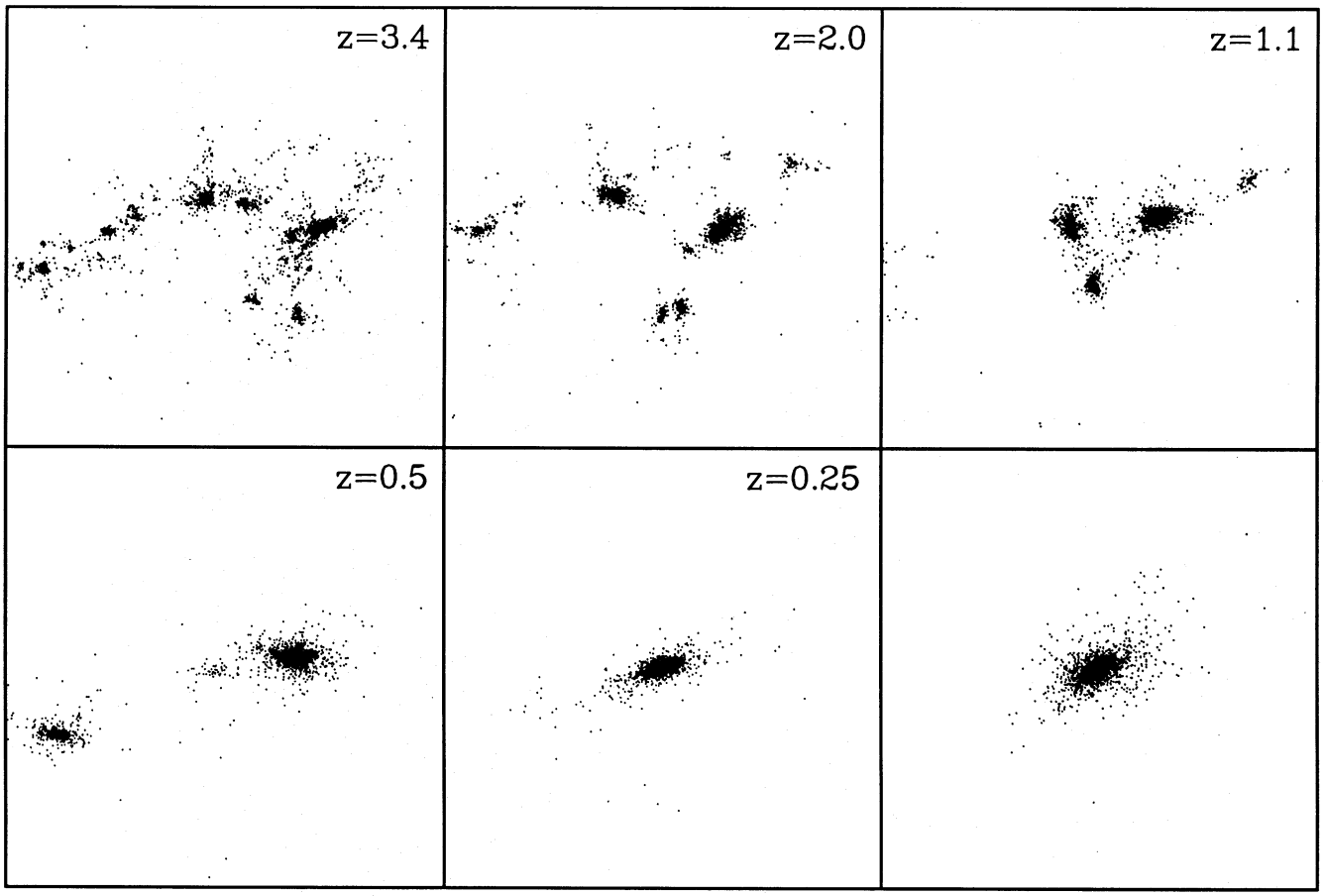

Figure 5. *N*-body simulation showing the formation of a massive cD-like galaxy in the centre of a rich cluster (kindly provided by Ray Carlberg). This has been extracted from a larger million-particle simulation of a CDM universe (see Carlberg 1994 for details). Only those particles that end up in the final galaxy are shown. Each box is $\sim 4\ h^{-1}$ Mpc on a side, and the redshift is shown in the upper right corner. Note the highly anisotropic nature of the merger process, and how this is reflected in the shape and orientation of the galaxy at both low and high redshifts.

2.4 An illustration

A picture being worth a thousand words, Fig. 5 provides an illustration of the various points discussed above. Shown here is an *N*-body simulation of the formation of a massive cD-like galaxy (kindly provided by Ray Carlberg) which was extracted from a larger million-particle simulation of the formation of a rich Coma-like cluster in a CDM universe (see Carlberg 1994). Fig. 5 shows the distribution of only those particles that end up in the final BCG at redshift $z = 0$, plotted at different stages during the formation process.

What is abundantly clear is that this galaxy forms not from the monolithic collapse of a single uniform-density perturbation, but rather via a series of mergers involving progressively larger clumps. Most importantly, these mergers do not occur in a random, isotropic manner; rather, the merger process is highly *anisotropic*, with the predominant direction reflecting the presence of a local large-scale filamentary feature in the matter distribution. The BCG shown in Fig. 5 is quite prolate throughout most of its lifetime, even at redshifts $z \gtrsim 3$. The orientation of the major axis of the galaxy reflects its anisotropic formation history; it is well aligned with the major axis of the cluster in which it resides and its orientation is little changed over its lifetime.

It is important to emphasize again that the development of filamentary structures and the formation of BCGs by anisotropic mergers is *not* unique to CDM; a similar formation scenario is likely to occur in *many* hierarchical clustering models, especially those originating from relatively flat initial density fluctuation spectra.

2.5 The link between BCG properties and large-scale structure

An anisotropic merger model for the formation of brightest cluster galaxies can successfully account for a number of their observed properties.

(1) *BCG alignments with larger scales.* The model presented here offers a straightforward explanation for the correlation between BCG orientations on kpc scales and the surrounding distribution of matter on scales of Mpc and tens of Mpc. Built up by a series of mergers which occur along preferred directions, the major axes of BCGs inevitably develop orientations which mirror that of their parent cluster and the surrounding filamentary pattern of superclustering. Stellar systems have long dynamical memories, and hence these BCGs retain their preferred orientations over a Hubble time, even after the merger frequency declines at recent epochs. Note that this model can explain why even the innermost regions of BCGs reflect the large-scale alignment tendency; *N*-body simulations demonstrate that in head-on mergers the final orientation of the post-merger product is communicated all the way to the core (Villumsen 1983 and references therein). An analogous anisotropic formation process presumably also occurs for clusters of galaxies, as subclusters fall together radially along filaments.

It is interesting to speculate that BCG alignments might have been even stronger at high redshifts compared to today. The majority of mergers which BCGs are likely to undergo at low redshifts are via cannibalism of smaller galaxies brought to the cluster centre by dynamical friction. Because this process tends to circularize the orbits of the infalling galaxies, mergers at recent epochs will be much more isotropic than in the past, and thus will dilute what was perhaps initially a stronger BCG alignment tendency.

(2) *The shapes of BCGs.* As mentioned earlier, brightest cluster galaxies are generally quite flattened in appearance. The distribution of observed BCG ellipticities indicates that they are most probably intrinsically prolate in shape (Porter et al. 1991; Ryden et al. 1993). In particular, Ryden et al. (1993) find that BCGs tend to be significantly flatter and more prolate than other cluster members, which they interpret as an indication that BCGs have a special formation history.[4] The anisotropic merger model proposed here naturally predicts that BCGs will have strongly prolate shapes. This formation scenario might also explain Leir & van den Bergh's (1977) observation that the most dominant BCGs tend to have the most elongated shapes; presumably such galaxies were built up by an exceptional number of mergers of material streaming along filaments.

(3) *Anisotropic velocity dispersions.* It is well known that the flattened shapes of BCGs, and elliptical galaxies in general, are supported not by rotation, but rather by an anisotropic velocity dispersion. In fact, kinematic observations indicate that the most luminous elliptical galaxies, particularly BCGs, have the least rotation (Davies et al. 1983; Carter et al. 1985). A strongly anisotropic velocity dispersion would arise quite naturally in the BCG formation model described here, as the proto-BCG fragments fall together along predominantly radial orbits.

2.6 A case study: Abell 1656 (Coma)

How realistic is the anisotropic merger model for BCG and cluster formation proposed here? As an illustrative example, let us consider what is widely regarded as the 'quintessential' rich cluster, Abell 1656 (Coma).

The Coma cluster and its environs are among the best studied regions in the sky. Coma resides in a prominent supercluster at $z \approx 0.02$ whose total extent is $\sim 100\ h^{-1}$ Mpc or more. As Fig. 6 shows, the galaxy distribution around Coma is clearly quite filamentary in appearance, with thin, quasi-linear features extending over large portions of the sky. Seen in projection, the dominant filamentary feature in which Coma is embedded lies along a position angle of roughly 70°–80°. Coma's nearest neighbour, Abell 1367, lies 22 h^{-1} Mpc away and is connected by a narrow bridge of galaxies (Gregory & Thompson 1978; de Lapparent et al. 1986).

As the lower three panels of Fig. 6 reveal, *the shape and orientation of both the Coma cluster and its brightest member galaxy clearly reflect these large-scale anisotropies in the surrounding matter distribution.* The projected distribution of Coma member galaxies (Fig. 6, lower centre panel) is obviously quite flattened, with the cluster major axis oriented in position angle $\sim 80°$ (West 1989 and references therein). *Einstein* observations of the hot X-ray-emitting gas (Fig. 6, lower left panel), which should provide the most reliable tracer of Coma's mass distribution, also indicate a major-axis orientation of $\sim 82°$–$88°$ (McMillan, Kowalski & Ulmer

[4]Ryden et al. (1993) measured shapes only for radii less than 10 h^{-1} kpc. Because BCGs become flatter at larger radii, they differ even more strongly from normal ellipticals than is suggested by their analysis.

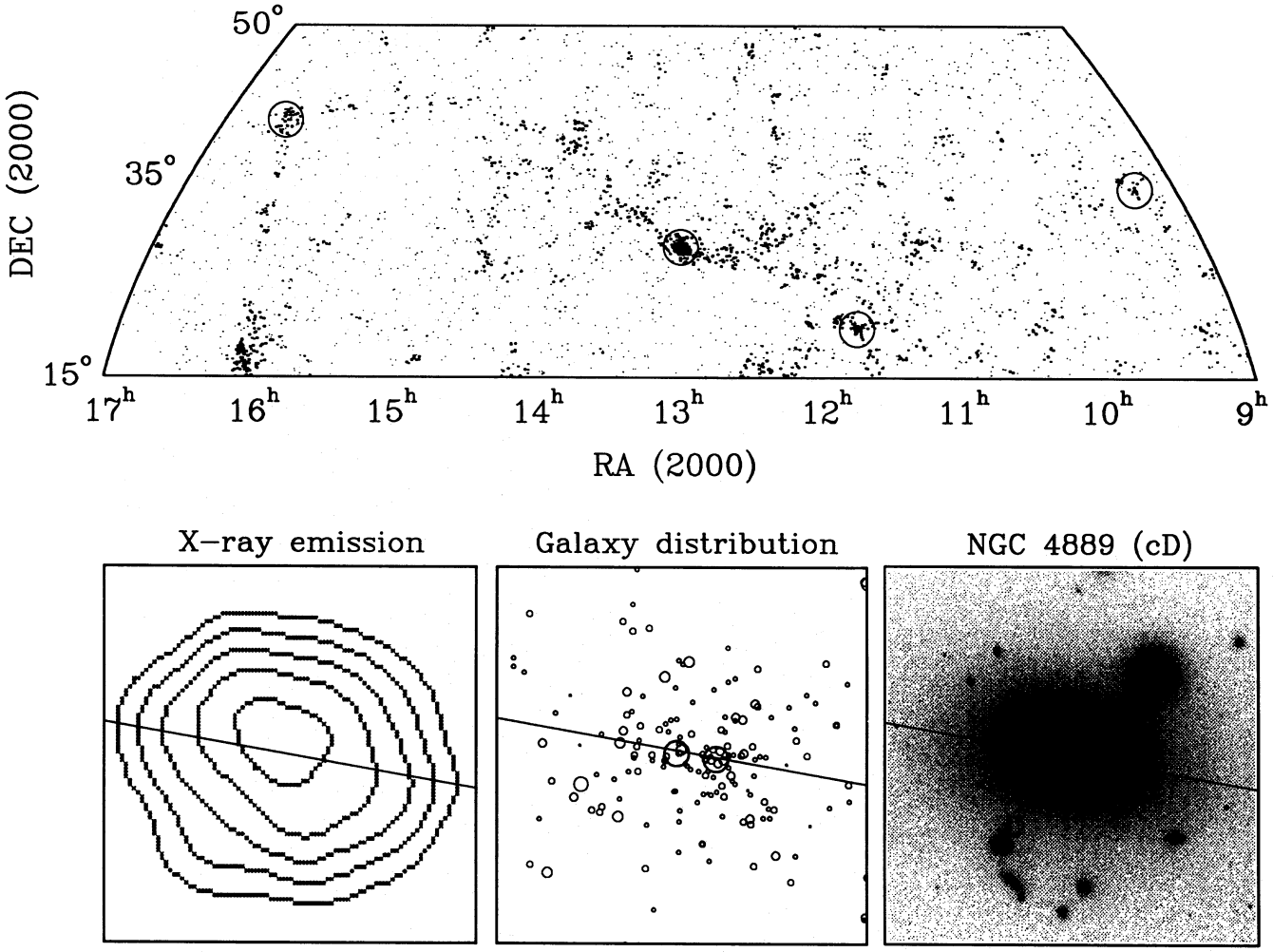

Figure 6. The Coma cluster in relation to its surroundings. The upper panel shows the distribution of 3649 galaxies contained in the RC3 (de Vaucouleurs et al. 1991), centred on Coma (RA = 12^h59^m, Dec. = 27° 58′). To highlight features in the galaxy distribution, symbol sizes are proportional to the logarithm of the local density around each galaxy, determined by counting the number of neighbouring galaxies within a projected radius of 1°. Circles denote Abell clusters with redshifts $z \leq 0.03$ (in order of increasing right ascension: Abell 779, 1367, 1656 and 2197/2199). The lower left-hand panel shows contours of the density distribution of hot X-ray-emitting gas in Coma, as mapped by the *Einstein* X-ray satellite. The field of view is $\sim 1\ h^{-1}$ Mpc across (north is up and east to the left). The lower middle panel shows the distribution of 160 Coma member galaxies within $\sim 0.7\ h^{-1}$ Mpc of the cluster centre (data are from Mazure et al. 1988). Symbol sizes are proportional to the galaxy size measured at the $b = 26.5$ magnitude isophote. The two giant galaxies are the elliptical pair NGC 4874 and 4889. The lower right-hand panel shows a grey-scale image of the brightest cluster galaxy NGC 4889 (kindly provided by Jim Schombert). The field shown is 60 h^{-1} kpc across. In each of the lower panels, the solid line denotes the overall cluster major axis, in position angle 80°.

1989; Buote & Canizares 1992). This can be seen even more clearly in recent high-resolution *ROSAT* images (White, Briel & Henry 1993). Hence the principal axis of the Coma cluster shares the same general orientation as that of the surrounding matter distribution on scales of tens of Mpc. Coma's major axis 'points' along the local filament in which it is embedded, in the direction of its nearest neighbouring cluster, Abell 1367.

This alignment effect continues to even smaller scales. Coma is the prototype of Rood–Sastry (1971) B-type clusters, which possess *two* dominant galaxies that are very much brighter than any other cluster members. NGC 4889 and 4874 are a pair of giant ellipticals in the centre of Coma whose projected separation is $\sim 150\ h^{-1}$ kpc. The separation vector between these two galaxies lies along a position angle of 80°, and thus is identical to the orientation of the cluster major axis. It has been suggested by a number of authors that NGC 4889 and 4874 each reside in distinct subclusters which may have recently fallen together to form the Coma cluster (Fitchett & Webster 1987; Mellier et al. 1988; White et al. 1993).

The cD galaxy NGC 4889 is the brightest member of Coma (Fig. 6, lower right panel). It is quite elongated in appearance, with its major axis oriented along a well-defined position angle of 80° which remains unchanged over radii from $\sim 300\ h^{-1}$ pc to $20\ h^{-1}$ kpc from the galaxy centre (Fig. 7). Hence even the very innermost sub-kpc regions of NGC 4889 are aligned with its surroundings on scales of tens of Mpc. The second-brightest galaxy, NGC 4874, shows no obvious alignment tendency.

These various observations suggest a picture in which the Coma cluster and its BCG were built up by mergers of

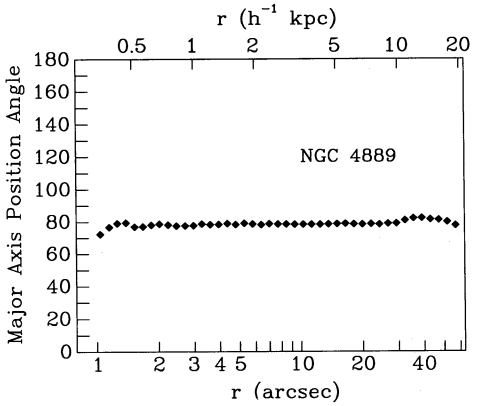

Figure 7. The major-axis orientation of NGC 4889 as a function of radius (from data published by Jorgensen, Franx & Kjaergaard 1992).

material which infell along a preferred axis defined by the prominent filamentary feature seen in Fig. 6. Direct dynamical evidence that material continues to stream along high-density ridges into the Coma cluster has recently been provided by Bothun et al. (1992). Coma is not unique; numerous other examples of BCGs aligned with their parent clusters and local large-scale structures can be found (see e.g. West & Schombert, in preparation).

To summarize the picture thus far, BCGs (and their parent clusters) are formed via highly anisotropic mergers. The ordered nature of this formation process imprints a preferred orientation on these galaxies which mirrors anisotropies in the surrounding matter distribution on much larger scales. This is the origin of the BCG alignment effect seen in Fig. 2. This model is similar in spirit to van den Bergh's (1983) suggestion that BCGs are the 'proto-nuclei' of rich clusters.

3 HIGH-REDSHIFT RADIO GALAXIES AS THE PRECURSORS OF BCGs

Matthews, Morgan & Schmidt (1964) first pointed out that many of the most powerful radio sources at low redshifts are associated with cD galaxies. It therefore seems reasonable to presume that extremely powerful radio galaxies at high redshifts may have been the progenitors of BCGs seen today. This hypothesis is supported by a number of observational and theoretical arguments.

(1) Observational studies of the environments of radio galaxies and radio-loud quasars at redshifts $0.5 \lesssim z \lesssim 1$ have provided direct evidence that these objects generally reside in dense regions comparable to Abell clusters (Yee & Green 1987; Yates, Miller & Peacock 1989; Hill & Lilly 1991; Bahcall & Chokshi 1991, 1992).

(2) Mergers and interactions have long been implicated as playing an important, if not paramount, role in triggering radio activity in low-redshift galaxies (e.g. Baade & Minkowski 1954; Balick & Heckman 1982; Hutchings, Crampton & Campbell 1984; Heckman et al. 1986). It seems quite likely that similar processes may have been responsible for the creation and fuelling of the first generation of powerful radio sources at high redshifts. Indeed, high-resolution CCD images of distant radio galaxies give the strong impression that many of them are in the throes of merging with companions. If radio activity is triggered by interactions and mergers, then the most probable locations of radio galaxies at high redshifts would be in dense environments, particularly the cores of developing protoclusters.

(3) It is well established that the most powerful nearby radio galaxies are generally associated with giant elliptical galaxies, often BCGs, having typical masses of $\gtrsim 10^{12}$ $M_\odot$ (e.g. Cyg A, Her A, Cen A, etc.). The *K*- and *R*-band magnitudes of distant radio galaxies suggest that they are equally massive systems (Lilly & Longair 1984; Lilly 1990). It seems reasonable to expect that the most massive galaxies at high redshifts (powerful radio galaxies) were the ancestors of the most massive galaxies in the low-redshift Universe (BCGs).

(4) Order-of-magnitude estimates indicate that the space density of powerful radio galaxies and quasars at high redshifts was comparable to the present space density of cD galaxies. Dunlop & Peacock (1990) derived a comoving number density of $\simeq 10^{-7}\ h^3$ Mpc^{-3} for powerful 3C-type radio galaxies out to redshifts $z \simeq 2$–4; however, given the expected short lifetimes of radio sources ($\lesssim 10^8$ yr), the true number of such objects could be significantly higher than this estimate. For comparison, the space density of $R \geq 1$ Abell clusters is $\sim 7 \times 10^{-6}\ h^3$ Mpc^{-3} (Bahcall & Soneira 1983; Peacock & West 1992), although only ~ 20 per cent of these contain a dominant cD-like galaxy (Struble & Rood 1987). Although these estimates are rather crude, the rough agreement between the space densities of high-z radio galaxies and low-z BCGs is consistent with them being the same population of objects seen at different evolutionary stages.

(5) Given an assumed form of the primordial power spectrum of density fluctuations, it is possible to predict the expected space density of galaxies and clusters as a function of epoch. Efstathiou & Rees (1988), using the analytic theory of Press & Schechter (1974), calculated an expected comoving space density of $\sim 10^{-6}$ Mpc^{-3} for $\sim 10^{12}$-$M_\odot$ galaxy haloes at $z \simeq 4$ in the CDM cosmogony (however, these numbers are sensitive to the assumed normalization of the power spectrum). Hence theoretical considerations suggest that at least some BCG-like galaxies are likely to have already existed at the redshifts of the most distant observed radio galaxies. Similar arguments for the early formation of the massive host galaxies of quasars have been given by Turner (1991). The most likely sites for the formation of the first generation of galaxies would have been in the dense cores of protoclusters, where protogalaxies would collapse on a significantly shorter time-scale than objects of comparable mass in lower density environments. Hence BCGs would probably have been amongst the earliest galaxies.

While no single argument offers incontrovertible proof of a connection between high-redshift radio galaxies and low-redshift BCGs, taken together the evidence for such a link is rather compelling. If such a connection exists, then the physical processes involved in the formation of BCGs may also have influenced the properties of these powerful radio sources. Having argued in previous sections that highly anisotropic mergers will produce prolate BCGs that have preferred orientations built into them, the effect of such a formation history on the genesis of radio galaxies is considered in the following sections.

4 WHAT DETERMINES THE JET ORIENTATION IN POWERFUL RADIO GALAXIES?

4.1 The fate of infalling gas

At early epochs, mergers of smaller gas-rich subunits and accretion of surrounding material are likely to provide an abundant source of cold gas in burgeoning young BCGs. What is the fate of this gas?

Many authors have argued that *cold gas falling into a spheroidal galaxy will invariably settle into a thin disc whose angular momentum vector is aligned with one of the principal axes of the galactic mass distribution* (e.g. Kahn & Woltjer 1959; Gunn 1979; Tubbs 1980; Tohline, Simonson & Caldwell 1982; van Albada, Kotanyi & Schwarzschild 1982; Steiman-Cameron & Durisen 1988). This conclusion is based on the following chain of reasoning.

(i) Collisions between infalling gas clouds will quickly dissipate random motions; whatever net angular momentum the gas has will cause it to settle into a disc which rotates about the centre of mass of the galaxy.

(ii) Gas in equilibrium in an axisymmetric gravitational potential must move in closed, non-intersecting orbits that lie in the symmetry plane of the galaxy. This is because in a non-spherical, axisymmetric potential any gas cloud whose orbit is inclined to the symmetry plane of the mass distribution will experience a gravitational torque. This torque will cause the gaseous disc to precess until eventually its angular momentum vector is aligned with the axis of symmetry of the galaxy.

(iii) Differential precession of the disc causes a smooth, continuous twist to develop as gas at different distances from the galactic centre settles into the equilibrium plane on different time-scales. Collisions between gas clouds in adjacent orbits lead to efficient dissipation, and consequently the reorientation of the disc involves a loss of angular momentum which drives gas towards the centre of the galaxy.

(iv) Regardless of whatever initial orientation the angular momentum vector of the infalling gas had, the final orientation of the gaseous disc is determined *solely* by the shape of the galaxy mass distribution. It is straightforward to show that if the gravitational potential is *prolate* then the disc spin axis will precess until it is aligned with the *major* axis of the galaxy, while in an *oblate* galaxy the angular momentum vector of the disc will coincide with the *minor* axis.

The time required for infalling gas to settle into this preferred plane is somewhat uncertain. In the first phase, collisional damping of random motions between gas clouds will lead to the formation of a gaseous disc on the order of a dynamical time, $\sim 10^8$ yr. The time-scale for this disc then to reorient itself into an equilibrium configuration within the galaxy depends sensitively on four factors: (1) the initial degree of misalignment between the angular momentum vector of the disc and the symmetry axis of the galaxy; (2) the shape of the galactic potential; (3) the viscosity of the gas and the efficiency of the dissipative forces at work, and (4) the distance from the galactic centre.

Analytic estimates of the disc settling time, τ_s, have been derived by a number of authors using different assumptions (e.g. Gunn 1979; Tohline et al. 1982; Steiman-Cameron & Durisen 1988). The predicted settling times vary by factors of a few, but a characteristic value is $\tau_s \simeq 10^9$ yr. Numerical simulations using a variety of techniques also suggest upper limits of $\tau_s \simeq 10^9$ yr for gas at a distance of ~ 10 kpc from the centre of a large elliptical galaxy to settle into the symmetry plane, and perhaps as little as 10^8 yr nearer to the galactic centre (Tubbs 1980; Tohline et al. 1982; Habe & Ikeuchi 1985; Steiman-Cameron & Durisen 1988; Christodoulou & Tohline 1993). Note, however, that in the anisotropic merger model of BCG formation proposed here the infalling gas at high redshifts is presumed to arrive with little initial angular momentum, and the host galaxy is presumed to be quite elongated in shape, so the time-scale for the gaseous disc to settle into the preferred plane could be significantly shorter than the above estimates, perhaps by as much as a factor of 5 to 10 (see Christodoulou & Tohline 1993).

4.2 Radio source production

Since the pioneering works by Salpeter (1964), Lynden-Bell (1969) and Blandford & Rees (1974), the standard model for nuclear activity in galaxies has envisaged a massive compact object, usually a black hole of order $\sim 10^7$–10^9 $M_\odot$, which acts as a central engine in the production of radio emission (see Begelman, Blandford & Rees 1984 or Blandford 1990 for a review). In this picture, the radio power is derived from twin collimated beams of relativistic material which are ejected along the black hole spin axis. The total energy output of the active galaxy, $L_{\rm tot}$, is related to both the mass of the central black hole, $M_{\rm bh}$, and the mass deposition rate, $\dot{m}$. The maximum source luminosity is set by the Eddington limit,

$$L_{\rm tot} \simeq 1.3 \times 10^{46} \left(\frac{M_{\rm bh}}{10^8\ {\rm M}_\odot} \right) {\rm erg\ s^{-1}}, \tag{9}$$

and the required accretion rate is

$$\dot{m} \simeq \left(\frac{0.1}{\epsilon} \right) \left(\frac{L_{\rm tot}}{10^{46}\ {\rm erg\ s^{-1}}} \right) {\rm M_\odot\ yr^{-1}}, \tag{10}$$

where ϵ is the efficiency of mass–energy conversion, usually assumed to be $\epsilon \lesssim 0.1$. Hence to produce powerful 3C radio galaxies with luminosities $L_{\rm tot} \gtrsim 10^{46}$–$10^{47}$ erg s^{-1} requires a minimum black hole mass of $\sim 10^8$–10^9 $M_\odot$ and accretion rates of a few $M_\odot$ yr^{-1} of infalling gas.

In the picture described in Section 4.1 for the fate of cold gas falling into a galaxy or protogalaxy, the outward transport of angular momentum as the gaseous disc precesses and aligns itself with the symmetry axis of its host galaxy will cause material to infall slowly towards the centre of the galaxy. This led Gunn (1979) to propose that such a process could provide a natural and efficient means of fuelling a black hole lurking in the galactic nucleus ('feeding the monster' in Gunn's terminology), and in fact this mechanism could also be responsible for its formation. Rees (1978) similarly suggested that 'Black holes may develop from an accumulation of gas with the same provenance as that which later fuels the accretion process.'

An important consequence of such a scenario for black hole formation is that the orientation of the black hole spin axis will be strongly coupled to its surroundings. This conclusion is based on the following considerations. If the black

hole formed from gas that accumulates at the centre of the host galaxy in the manner envisioned by Gunn (1979), then its spin axis at birth would presumably reflect the angular momentum vector of the progenitor accretion disc, which, based on the arguments in the previous subsection, is determined by the host galaxy geometry. However, even if the black hole initially formed with some randomly oriented spin axis (or was captured by the BCG from another galaxy), as the fuelling accretion disc dumps more and more material on to the central engine each unit mass of accreted material alters the net angular momentum of the black hole, and consequently its spin axis would slowly precess until it eventually aligned with the spin axis of the accretion disc (Rees 1978). The time-scale for this realignment to occur will of course depend on the original black hole angular momentum, the mass deposition rate, and the initial misalignment between the black hole and accretion disc spin axes; to first order

$$t_{\rm align} \simeq \left(\frac{M_{\rm bh}}{\dot{m}}\right)\left(\frac{J}{J_{\rm max}}\right)\left(\frac{r_{\rm S}}{r_{\rm LT}}\right)^{1/2}, \qquad (11)$$

where J is the angular momentum of the black hole, $J_{\rm max}$ is the maximum angular momentum of a Kerr black hole, $r_{\rm S}$ is the usual Schwarzschild radius and $r_{\rm LT}$ is the radius at which the relativistic Lense–Thirring effect becomes important (Bardeen & Petterson 1975; Rees 1978). Typically, one would expect the black hole to realign itself with respect to the fuelling accretion disc on a time-scale $t_{\rm align} \simeq 10^8$ yr (Rees 1978).

It therefore follows that, in the picture of galaxy and black hole formation described here, the orientations of the black hole spin axis and hence the radio jets are inextricably linked to the formation of the galaxy itself.[5] As a consequence, the radio jets will inevitably align with one of the principal axes of the host galaxy, depending on the geometry of its mass distribution. This important point has been made previously by a number of other authors; for example, Tohline et al. (1982) concluded that 'all radio jets in elliptical galaxies should align with a principal axis of the galaxy. Radio jets should align with the projected *major* axis of prolate ellipticals, and they should align with the projected *minor* axis of oblate ellipticals.'

Observational evidence strongly supports the above theoretical arguments. A number of nearby elliptical galaxies are observed to contain gas or dust lanes, presumably obtained from recent mergers with small gas-rich companions. In the majority of cases these discs are aligned with the major or minor axis of the galaxy, with the radio jets emanating perpendicular to the dust lanes (Bertola & Galletta 1978; Kotanyi & Ekers 1979; Hawarden et al. 1981; see Bertola 1992 for a recent review). The prototype of this class of objects is Centaurus A (NGC 5128), whose dust lane is observed to lie along the minor axis of the galaxy, and whose radio jet is clearly aligned with the galaxy major axis (Tubbs 1980). Recent *HST* observations by Jaffe et al. (1993) have provided dramatic evidence of an accretion disc fuelling the central engine in the Virgo cluster galaxy NGC 4261 (3C 270). Hence it appears that in many nearby elliptical galaxies there is a fundamental physical connection between the orientation of the radio jets, the gaseous accretion disc, and the galaxy geometry. Indeed, it has frequently been argued that the orientations of dust lanes and radio jets in nearby elliptical galaxies might be used to discriminate between oblate, prolate and triaxial intrinsic galaxy shapes.

[5]While this scenario for imparting a preferred orientation to the black hole spin axis is arguably the most natural, other possibilities also exist. For example, mergers that occur preferentially in a single direction might over time exert a sufficient torque to cause a precession of the black hole spin axis (e.g. Begelman, Blandford & Rees 1980; Wirth, Smarr & Gallagher 1982).

4.3 The alignment effect in high-redshift radio galaxies

Assuming that high-redshift radio galaxies are proto-BCGs, then according to the formation model described in Section 2 they are likely to be quite *prolate* in shape, even at the earliest stages of their formation (see Fig. 5). *Consequently, infalling gas will quickly settle into an accretion disc whose angular momentum vector is aligned with the major axis of the galaxy mass distribution, and hence an alignment between the radio jets and the galaxy major axis is expected.* In this picture, then, the observed alignment effect in high-redshift galaxies (Fig. 1) has a purely *dynamical* origin, with the optical, infrared and radio jet orientations reflecting the underlying mass distribution in these (proto)galaxies.

It is important to emphasize that the model proposed here does not preclude the possibility that some fraction of the aligned light may have its origin in jet-induced star formation or scattering. The fact that polarization is observed in high-z radio galaxies clearly indicates that some amount of scattering is occurring. Likewise, the bluer colours of some high-redshift radio galaxies relative to their low-redshift counterparts are suggestive of recent star-forming activity. Indeed, it is entirely possible that there may be two distinct forms of the alignment effect. While the merger model provides a natural explanation for radio galaxies such as 3C 114, 265 and 356, which show spectacular elongations (and clumpiness) in both the optical and infrared, it may have some difficulty explaining those cases, such as 3C 194, 266 and 352, in which the blue light is observed to be highly elongated but there is no corresponding extension in the infrared. Nevertheless, if many of the most powerful radio sources at high redshifts are indeed proto-BCGs, as the arguments presented in Section 3 suggest, then the *dominant* effect is likely to be the *intrinsic* alignment of the radio jets with the galaxy mass distribution. In this case, scattering and starbursts are only second-order effects which may act to enhance further the alignments with the radio axis. In a sense, one should view the merger model proposed here as the antithesis of jet-induced star formation models for the alignment effect – in the latter, it is the radio jets that influence the distribution of stellar light in these galaxies, whereas in the merger model it is the stellar distribution that dictates the orientation of the radio jets!

4.4 Dependence of the alignment effect on radio power

Dunlop & Peacock (1993) have recently shown that the radio–infrared (and possibly optical) alignment effect is strongly dependent on radio power. By comparing two samples, which were matched in redshift ($0.8 \leq z \leq 1.3$) but

had radio powers that differed by an order of magnitude, these authors found that, while the most powerful radio galaxies showed a clear alignment effect, no alignments were seen for the weaker radio galaxies. From this they deduced that radio power, rather than redshift, is the primary factor behind the apparent epoch dependence of the alignment effect, since it is the most powerful radio galaxies that are invariably selected at high redshifts. On the basis of these and other observations they argued in favour of scattering models for the origin of the alignment effect.

A correlation between radio luminosity (or redshift) and the strength of the alignment effect could, however, also arise quite naturally in the merger model proposed here. Recall two important observed characteristics of BCGs at low redshifts: (1) they are the *only* galaxies that exhibit any tendency to be aligned with their surroundings, and (2) they have significantly flatter and more prolate shapes than other elliptical galaxies. This suggests that normal ellipticals formed in a rather more mundane manner than the highly anisotropic mergers envisaged here for the formation of BCGs in the centres of rich clusters.

Observational evidence and theoretical arguments suggest that the majority of elliptical galaxies are neither strongly prolate nor oblate in shape, but most probably *triaxial* (e.g. Binney 1978; Peacock & Heavens 1985; Bardeen et al. 1986; de Zeeuw & Franx 1991; Fasano & Vio 1991; Warren et al. 1992). In triaxial galaxies *two* families of stable orbits are possible, in the planes perpendicular to the longest and shortest axes, and hence there is no single preferred plane for a gaseous accretion disc to settle into (e.g. van Albada et al. 1982; Merritt & de Zeeuw 1983). Moreover, the principal axes of triaxial galaxies will not generally coincide with the observed major and minor axes of the projected light distribution. Consequently, based on the scenario for black hole formation described in Section 4.2, one would not expect to observe any clear alignment tendency between the radio, optical and infrared axes in most elliptical galaxies – *only the subset of radio galaxies corresponding to prolate (proto)BCGs should show a strong alignment tendency.*

A number of authors have argued on various theoretical grounds that the most massive galaxies are likely to contain the most massive central black holes (Soltan 1982; Efstathiou & Rees 1988; Small & Blandford 1992; Haehnelt & Rees 1993). The recent Haehnelt & Rees (1993) and Small & Blandford (1992) scenarios for black hole formation predict a strong epoch dependence of the characteristic black hole mass, with galaxies that form at lower redshifts possessing less massive black holes. If one makes the simple assumption that

$$M_{\rm bh} \propto M_{\rm gal} \tag{12}$$

and that the active galaxy is radiating at or near the Eddington limit, then equation (9) can be written

$$L_{\rm tot} \propto M_{\rm bh} \propto M_{\rm gal}. \tag{13}$$

Hence, provided there is an abundant supply of fuel during the active phase, a strong correlation between radio luminosity and host galaxy mass is expected.

It is evident from the above expression that a 10^{12}-$M_\odot$ BCG will have a radio luminosity that is roughly an order of magnitude greater than that of a 10^{11}-$M_\odot$ normal elliptical galaxy. *Consequently, the identification of distant galaxies based on their enormous radio powers introduces a strong bias which favours the selection of massive BCGs over the general elliptical galaxy population – at the highest redshifts, virtually all of the most powerful 3C sources are likely to be protoBCGs.* At redshifts greater than $z \simeq 1$, which is where the alignment effect becomes common, the great majority of 3C galaxies have radio luminosities $L_{\rm radio} \gtrsim 10^{45}$ erg s^{-1}. At redshifts $z < 0.5$, where no alignment effect is seen, 3C sources span 4 decades in radio power, with most being weaker sources than their high-z counterparts. It therefore seems reasonable to speculate that radio galaxies at all redshifts that have $L_{\rm radio} \gtrsim 10^{45}$ erg s^{-1} are likely to be BCGs. Note that this does not mean that *all* BCGs will have large radio luminosities; inefficient fuelling can make weak radio sources out of even the most massive central engines. Some examples of the alignment effect in extremely powerful radio galaxies at low redshifts are presented in Section 5.

It is therefore tempting to conclude that the weaker $z \simeq 0.8$–1.3 radio sources in the Dunlop & Peacock (1993) sample correspond to *normal* elliptical galaxies rather than to BCGs. As already discussed, such galaxies would not be expected to show any strong tendency for alignment of their radio, optical and infrared axes since they are presumably triaxial, rather than prolate, systems. The more powerful 3C galaxies that show alignments presumably correspond to (proto)BCGs. Some support for this contention is provided by Dunlop & Peacock's observation that the infrared images of their weaker radio galaxies are generally rounder than those of the more powerful 3C galaxies; this is consistent with the flatter shapes of BCGs compared to average elliptical galaxies at low redshifts.

A correlation between the alignment effect and radio power would therefore seem to be a quite plausible consequence of the model proposed in this paper. If black hole mass is correlated with host galaxy mass, then one would expect the strength of the alignment effect to increase with radio luminosity as a higher proportion of (proto)BCGs are selected.

4.5 Ages and morphologies of high-redshift radio galaxies

Any successful model of radio galaxy formation must be able to explain not only the radio–optical–infrared alignment effect, but also the elongated and clumpy shapes that are characteristic of these high-z objects. In scattering and starburst models for the radio–optical–infrared alignment effect, the clumpy nature of high-redshift radio galaxies is simply assumed to be an a priori condition; presumably these galaxies were surrounded by numerous dense gas clouds and it is only those that happen to lie along the radio jet axis that are illuminated. *Yet the high incidence of double- and multiple-component galaxies with separations of only a few kpc (e.g. 3C 65, 114, 265, 356 and 368) strongly suggests that these are in the process of merging in the direction defined by the radio axis.* For example, Dunlop & Peacock's (1993) infrared image of 3C 114 shows a collinear distribution of at least six distinct clumps. Similarly, multicolour observations of 3C 256 by Rigler et al. (1992) show a highly elongated and irregular galaxy composed of numerous peaks strung out along the radio axis. The appearance of these galaxies finds a natural explanation in the merger model proposed here (see also Section 4.7 below for a detailed discussion of 3C 356).

Based on the scenario described in Section 2, one would expect young proto-BCGs at high redshifts to be quite clumpy and elongated in shape, with the individual components distributed in a quasi-linear configuration over a large angular extent (see e.g. Fig. 5).

Another issue of great debate at present concerns the ages of high-redshift radio galaxies: are we witnessing the first major burst of star formation in these galaxies, or were the bulk of the stars in these objects already formed at much higher redshifts, perhaps $z_{\rm form} \gtrsim 5$–10? The anisotropic merger model proposed here requires only that relatively stable prolate BCG potentials exist $\sim 10^8$ to 10^9 yr earlier than the highest redshifts at which the alignment effect is observed, since this is the assumed time-scale for a gaseous disc to settle into a preferred plane within the host galaxy (Section 4). Assuming a conservative estimate of $\tau_s = 10^9$ yr, then a strong alignment between the radio and optical axes in the majority of 3C galaxies at $z \simeq 2$ requires that their formation was well underway by a redshift of at least $z_{\rm form} \equiv 3$ (assuming an Einstein–de Sitter cosmology with $h = 1$). Note, however, that this does not require that the *entire* galaxy has been formed by this early epoch; galaxy formation is likely to have been a lengthy process (see e.g. Fig. 5). A more severe limit is provided by very high-redshift galaxies such as 4C 41.17 at $z = 3.8$, which is the most distant example of the alignment effect. This redshift corresponds to an epoch when the Universe was only ~ 10 per cent of its present age, and hence to produce the observed alignment would require the formation of a stable prolate gravitational potential by $z_{\rm form} \simeq 10$ for a disc settling time of 10^9 yr. If, however, τ_s were 10^8 yr instead of 10^9 then even the most distant radio galaxies known at present would require formation redshifts of only $z \simeq 5$ in order to explain the alignment effect.

4.6 A case study: 3C 356

Is there any observational evidence to support the proposed link between the formation of radio galaxy central engines and the matter distribution on larger scales?

An interesting example is provided by 3C 356 at $z = 1.08$, which is one of the most thoroughly studied distant galaxies to date. 3C 356 is a bona fide high-redshift 'monster', having a total radio luminosity of nearly 5 times that of Cygnus A. Its radio lobes are separated by more than 300 h^{-1} kpc (see Fig. 8). Observations by McCarthy et al. (1987) and Le Fèvre et al. (1988) revealed that its optical continuum and emission-line gases have elongated and clumpy morphologies which are both extremely well aligned with the radio axis in position angle $\sim 160°$. What is unusual about this galaxy is that it is composed of two distinct components of roughly equal luminosity that lie along the radio axis, separated by $\sim 25\ h^{-1}$ kpc (Fig. 8). Subsequent observations showed a similar morphology in the infrared (Eales & Rawlings 1990; Eisenhardt & Chokshi 1990; Dunlop & Peacock 1993). Rigler et al. (1992) suggested that this secondary component might be a companion galaxy that has wandered into the jet path and been illuminated.

Crawford & Fabian (1993) have presented *ROSAT* X-ray observations of 3C 356 and its environment; these are reproduced in Fig. 8. The total X-ray luminosity of $\sim 2 \times 10^{44}$ erg s^{-1} is comparable to that of many Abell clusters at low redshifts, which suggests that 3C 356 resides in a distant rich cluster of galaxies. The X-ray contours, which presumably trace the cluster potential, are quite elongated in shape, and the major axis of the distribution of hot gas appears to be quite similar in orientation to that of the radio, optical and infrared structures of the 3C 356 galaxy. On the basis of rather limited spectral information, Crawford & Fabian concluded that 3C 356 is located in the most distant cooling flow yet discovered, and argued that the radio–optical–infrared alignments in 3C 356 can be explained as a consequence of electron scattering of light from an obscured quasar nucleus.

It is possible to propose a very different interpretation of 3C 356 based on the anisotropic merger model developed here: namely, that 3C 356 is an excellent example of a cD galaxy in the process of forming via anisotropic mergers in the centre of a distant cluster (or protocluster) of galaxies, and that the observed radio, optical, infrared and X-ray alignments reflect the principal axis of the parent cluster and the local large-scale density field. In other words, the alignments seen in 3C 356 are quite comparable to the alignments observed for low-redshift BCGs such as NGC 4889 (Fig. 6), with the addition that the radio axis also shares this preferred orientation. 3C 356 is presumably a prolate BCG whose radio jets reflect the preferred orientation that has been built into this galaxy by a history of anisotropic mergers.

4.7 Superclustering at high redshifts

The model of BCG and radio galaxy formation proposed here implies a fundamental connection between the orientations of powerful radio jets and the surrounding matter distribution on scales of Mpc and even tens of Mpc. In this picture, the radio axis reflects the orientation of the host BCG, which in turn reflects the orientation of its parent cluster and larger scale anisotropies on supercluster scales. Given that brightest cluster galaxies are observed to 'point' towards neighbouring Abell clusters at low redshifts (e.g. Fig. 2 and references cited in Section 1), it follows that one would also expect the radio emission from these galaxies to reflect a similar alignment tendency.

Observational evidence that such an alignment effect may indeed occur at high redshifts has been presented by West (1991a,b), who claimed that the radio axes of neighbouring radio galaxies and radio-loud quasars at $z \gtrsim 0.5$ exhibit a statistically significant tendency to 'point' towards one another over separations of up to $\sim 40\ h^{-1}$ comoving Mpc. An example is shown in Fig. 9.

The theoretical model described in the present paper provides a straightforward explanation for these observational results, and suggests the very exciting possibility of using the relative orientations of neighbouring radio sources at high redshifts as a proxy to study distant BCG alignments, thus providing an observational probe of large-scale structure in the early Universe. As discussed in Section 4.4, this alignment effect should be strongest for the most powerful radio sources, since these are most likely to be BCGs. It is interesting to speculate too that if 'unified' models for radio-loud active galactic nuclei are correct (see Antonucci 1993 for a review) then quasars may simply be distant BCGs whose major axes point along the line of sight, whereas radio galaxies are BCGs whose major axes lie near the plane of the sky.

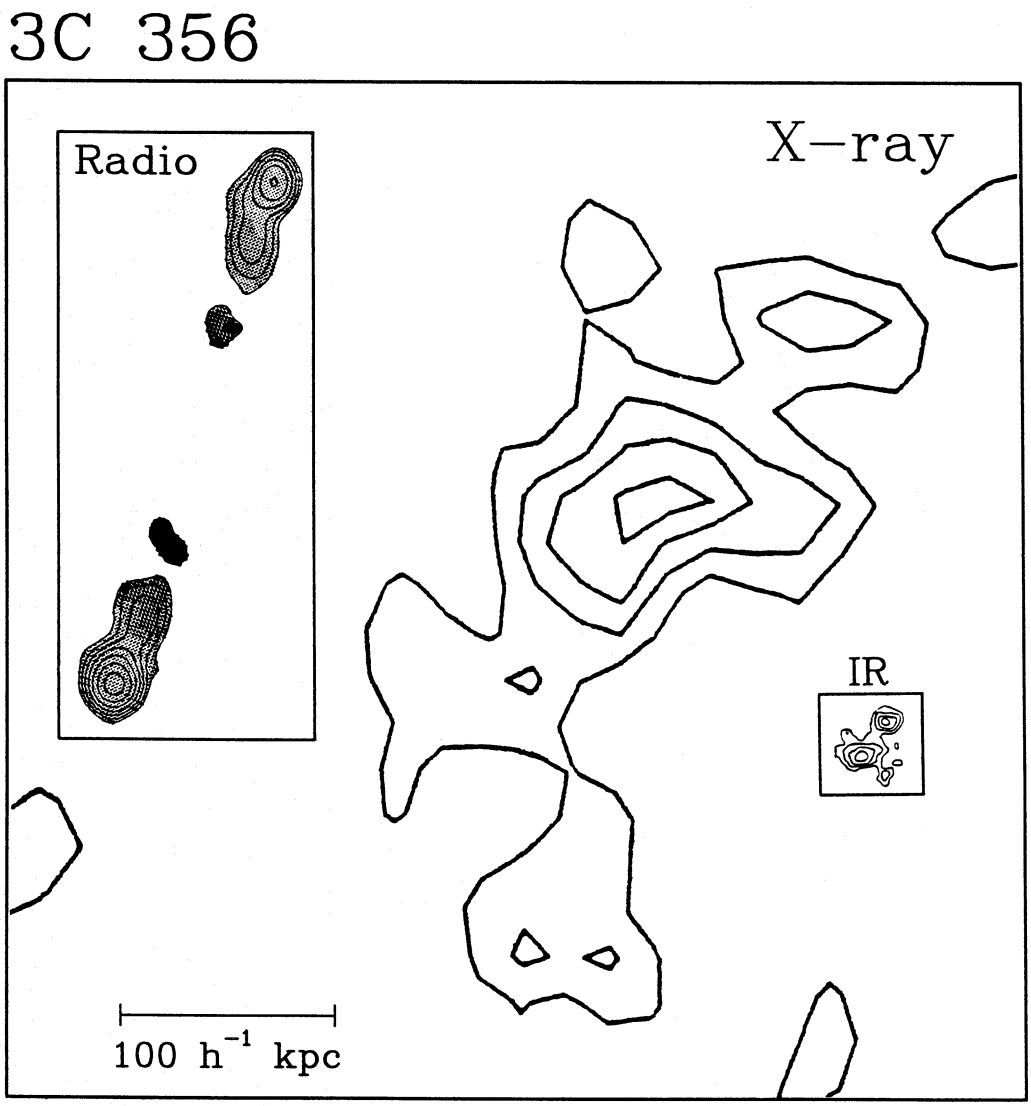

Figure 8. The alignment effect(s) in 3C 356. Shown here is a contour plot of the distribution of hot X-ray gas, as determined by Crawford & Fabian (1993) from *ROSAT* observations. The major axis of the X-ray emission extends over 0.5 h^{-1} Mpc. The insets show (approximately to scale) the radio structure of this galaxy at 151 MHz (taken from Leahy, Muxlow & Stephens 1989) and its infrared morphology (from Dunlop & Peacock 1993). The radio lobes are separated by more than 300 h^{-1} kpc; the separation between the two infrared clumps is only $\sim 25\ h^{-1}$ kpc. Note the clear overall alignment of the structure of the 3C 356 galaxy and its radio emission with the X-ray contours of its parent cluster.

5 LOW-REDSHIFT COUNTERPARTS TO HIGH-z RADIO GALAXIES

If the model of BCG/radio galaxy formation proposed here is correct, a crucial question that needs to be addressed is why no radio–optical–infrared alignment effect is seen at low redshifts.

To begin with, it is important to consider the existing observational data. To date, studies of radio jet orientations in nearby galaxies have invariably been based on samples composed primarily of *normal* (i.e. non-BCG) ellipticals. Recall from Sections 2 and 4, however, that *only* BCGs are expected to show any sort of alignment effect. As discussed in Section 4.4, identification of high-redshift galaxies on the basis of their extreme radio luminosities introduces a strong selection effect which favours BCGs over non-BCGs. The ubiquitous nature of the alignment effect at high redshifts is thus attributable to this selection effect, since the characteristic radio luminosities increase with redshift in a flux-limited sample such as the 3C catalogue, which means that one is observing an increasing fraction of protoBCG objects. At redshifts $z \lesssim 0.5$, on the other hand, 3C sources span a factor of 10 000 in radio power – some of these correspond to BCGs, but most do not.

The important question, then, is not whether low-redshift galaxies in general show the same radio–optical alignments seen in high-redshift galaxies, but rather whether BCGs in particular exhibit such alignments. Based on the anisotropic merger model developed here, one would expect that such alignments should occur (although see Section 5.3). Unfortu-

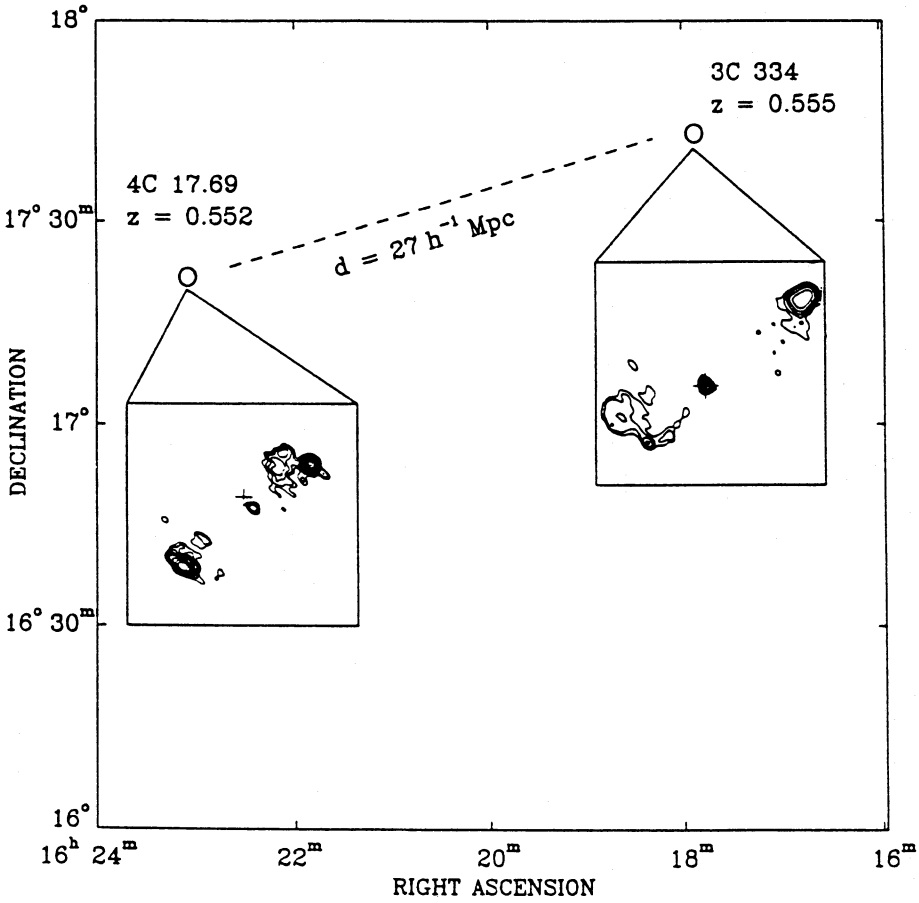

Figure 9. An example of a pair of aligned radio sources at high redshifts (from West 1991b).

nately, no comprehensive study of the relative orientations of BCG radio and optical axes has yet been carried out. However, a number of examples of low-redshift cD galaxies whose radio and optical structures are clearly aligned have been pointed out by West (1991a,b) and Andernach et al. (1993).

It is interesting to note that some of the most powerful radio galaxies at low redshifts *do* appear to have preferred orientations with respect to their surroundings, which suggests that they may indeed have formed in the manner proposed here. Some specific examples are discussed below.

5.1 Cygnus A (3C 405)

Cygnus A is generally considered to be the classic example of a Fanaroff–Riley type II (double-lobed) radio galaxy. It is by far the most powerful radio source in the low-redshift Universe, with a total radio luminosity in excess of 10^{45} erg s^{-1}. Its proximity affords a unique opportunity to study a nearby galaxy whose properties are likely to be quite similar to those of its high-redshift cousins.

The optical morphology of Cygnus A has been something of a puzzle ever since its discovery. The radio source is clearly associated with a cD galaxy at a redshift $z = 0.0565$, but, in their original observations of Cygnus A, Baade & Minkowski (1954) pointed out that 'in the center of this nebula are two bright condensations separated by 2″ in position angle 115°' and suggested that we may be witnessing a collision of two galaxies. Van den Bergh (1976) showed that these two components differ markedly, one being a source of continuum radiation while the other is dominated by emission-line radiation. Subsequent observations suggested that the double-nucleus appearance of Cygnus A is instead caused by a prominent dust lane which bisects the galaxy along its minor axis. The true nature of Cygnus A now appears by be somewhat more complex than even originally thought (see e.g. Stockton 1993 or Vestergaard & Barthel 1993 and references therein). Observations by Djorgovski et al. (1991) have revealed a bright infrared nucleus in Cygnus A, which they suggested may be a central quasar shrouded by dust, a contention that is supported by recent *HST* observations by Jackson et al. (1994).

The radio emission of Cygnus A has been mapped in numerous studies; the source has a well-defined radio major axis at position angle ~112° (e.g. Hargrave & Ryle 1974; Perley, Dreher & Cowan 1984). The radio jets are well collimated and show no evidence of any significant distortions before reaching the outer radio lobes at a projected distance of 50 h^{-1} kpc. *VLBI* observations (Carilli et al. 1991) show that the milliarcsec-scale (parsec) jet axis is extremely well aligned with the arcsec-scale (kpc) jet.

A striking feature of the radio and optical structures of Cygnus A is the similarity of their orientations. The principal axis of the radio emission has the same orientation as the apparent separation vector between the two optical clumps in the centre of the galaxy (or, equivalently, the radio jet is almost exactly perpendicular to the putative dust lane). Several independent pieces of evidence also suggest that both the radio and optical structures of Cygnus A are oriented quite close to the plane of the sky. Hargrave & Ryle (1974) and Dreher (1981) concluded on the basis of their observations of the radio hotspots that the angle between the radio source axis and the line of sight is probably $\sim 90° \pm 15°$. *VLBI* observations of the jet/counterjet ratio in Cygnus A are also consistent with an orientation close to the plane of the sky (Carilli et al. 1991). Optical observations further support this idea; Simkin (1977) concluded that the optical rotation axis of this galaxy is well aligned with the radio axis, and that both are inclined by $84° \pm 3°$ to the line of sight. These various results suggest a close connection between the orientations of the radio jets and the optical structure of Cygnus A (see Fig. 10).

Cygnus A is the dominant member of a cluster of galaxies, although the cluster's richness is difficult to ascertain because of its low galactic latitude ($b = 5°$). The Cygnus A cluster is detected as a bright X-ray source with a total X-ray luminosity of $\sim 6 \times 10^{44}\ h^{-2}$ erg s^{-1} extending over $1\ h^{-1}$ Mpc, which is typical of many Abell clusters (Arnaud et al. 1984; Edge et al. 1990). *Einstein* observations (Fig. 10) show that the distribution of hot X-ray gas, which presumably traces the cluster mass distribution, is clearly elongated in a position angle of $\sim 130°$. Hence the orientations of the optical structure and radio jets of Cygnus A on kpc scales are quite similar to the orientation of its parent cluster on Mpc scales.

A comparison of the position of the Cygnus A cluster with those of all Abell clusters reveals that Cygnus A lies only 21 h^{-1} Mpc from the rich cluster Abell 2319 (Fig. 11). This cluster has a mean redshift of $z = 0.0564$ based on velocities for 31 member galaxies (Struble & Rood 1991), which is practically identical to that of Cygnus A. Their relative proximity and similar redshifts suggest that Cygnus A and Abell 2319 probably belong to the same supercluster, whose orientation is quite close to the plane of the sky. *Most intriguingly, the radio jet of Cygnus A appears to 'point' directly at Abell 2319.* A great circle drawn from Cygnus A to A2319 lies along a position angle of 115°, which is the same orientation as the Cygnus A radio jet and the 'double nucleus' of the core (see Fig. 10).

One might, of course, be tempted to dismiss these various alignments as nothing more than mere chance. However, within the context of the model for cD/radio galaxy formation proposed here, these observations suggest the very real possibility that the orientation of the central black hole spin axis that powers Cygnus A 'remembers' its early formation history via anisotropic infall of material along this preferred axis of $\sim 115°$. In this picture, Cygnus A has accreted a gas-rich companion galaxy within the past 10^8–10^9 yr which is now fuelling this most recent burst of nuclear activity. In fact, it is interesting to speculate that the unusual structure of the innermost regions of Cygnus A might be at least partly attributable to transient features produced as the newly acquired gaseous disc and dust lane continue to settle into the symmetry plane of this galaxy.

5.2 Hercules A (3C 348)

Her A is another extremely powerful low-redshift ($z = 0.154$) radio galaxy. Like Cygnus A, it is a strong double-lobed radio source with narrow jets (Dreher & Feigelson 1984). The host galaxy of Her A is a very elongated cD galaxy in a cluster of galaxies (Owen & Laing 1989; Yates, Miller & Peacock 1989). Like Cygnus A, Her A also shows the same 'alignment effect' seen in its high-z cousins; its radio and optical major axes are well aligned along position angle $\sim 110°$ (see Fig. 12). This alignment of the radio jets with the galaxy major axis suggests that Her A is decidedly prolate in shape.

A comparison of the location of Her A with those of all Abell clusters reveals that it has two neighbouring rich clusters at nearly the same redshift (Fig. 12). Abell 2204 is an extremely rich (Abell richness class $R = 3$) cluster at $z = 0.152$ which lies 29 h^{-1} Mpc from Her A along a position angle of 98°. Abell 2210 ($z = 0.146$) is also located 29 h^{-1} Mpc from Her A along a similar position angle of 98°. *Hence the optical and radio axes of 3C 348 'point' to within ~ 10° of its nearest neighbouring Abell clusters.*

Recent optical imaging of Her A by Sadun & Hayes (1993) has shown that this galaxy has a double nucleus (previously thought to be a contaminating foreground star) with a separation of $\sim 10\ h^{-1}$ kpc between the two components. Interestingly, the relative position angle between the two nuclei is 135°, quite close to the overall orientation of the galaxy and its radio axis. This suggests that perhaps anisotropic merging along a preferred axis has occurred even quite recently for Her A.

5.3 Other examples

A number of cD galaxies in Abell clusters also show evidence of both alignment effects.

One example is the southern Parkes radio source PKS 2354−35. Schwartz et al. (1991) have presented a detailed discussion of this object. Although a much weaker radio source than Cygnus A and Her A discussed above (total radio luminosity $\sim 1.5 \times 10^{42}$ erg s^{-1}), it is associated with the cD galaxy in the rich southern cluster Abell 4059. This cluster is a bright X-ray source ($L_x \simeq 2 \times 10^{44}$ erg s^{-1}). PKS 2354−35 clearly exhibits a strong alignment between its optical and radio axes (position angles 155° and ~160°, respectively), which are also aligned with the optical and X-ray major axes of the parent cluster Abell 4059 (position angles 140° and 163°). Furthermore, this preferred radio–optical–X-ray axis of PKS 2354−35 and its parent cluster is closely aligned with the direction from Abell 4059 to its two nearest neighbour clusters; Abell 2717 lies only 12 h^{-1} Mpc along a position angle of 135°, while Abell 2660 is separated by 28 h^{-1} Mpc along a position angle of 164° relative to Abell 4059.

A similar example is provided by NGC 708, which is the brightest galaxy in Abell 262 and a rare example of a BCG with a dust lane (see Fig. 13). Kotanyi & Ekers (1979) noted that this dust lane is oriented nearly perpendicular to the radio source axis, the latter having a position angle of 76° (Parma et al. 1986; Baum et al. 1988). For comparison, the optical major axis of NGC 708 has a position angle of 48° (Binggeli 1982; Struble & Peebles 1985). The Abell 262

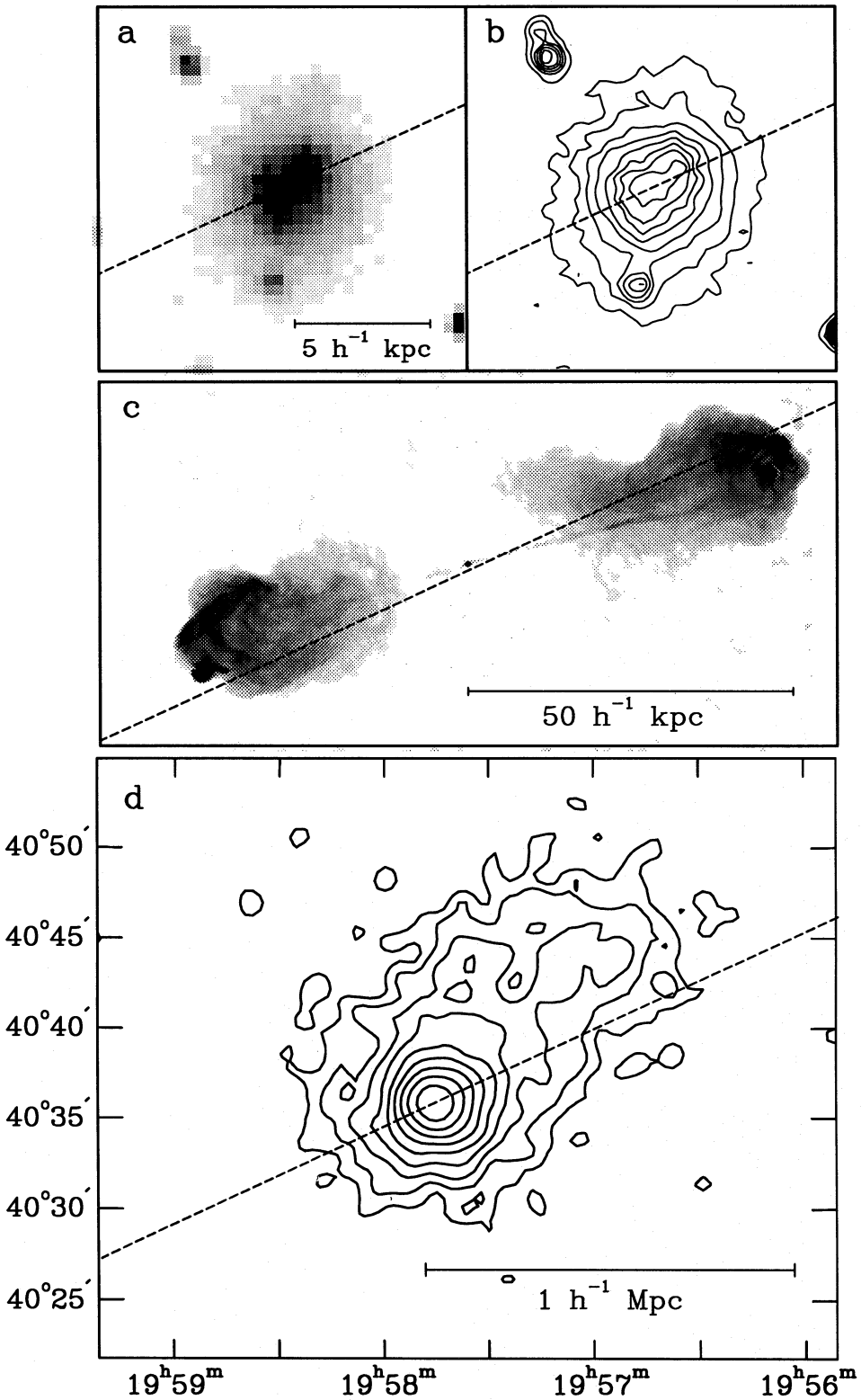

Figure 10. Optical, radio and X-ray morphologies of Cygnus A and its parent cluster. The four panels show (a) an *I*-band CCD image of Cygnus A (kindly provided by Jim Schombert); (b) a contour plot of the *I*-band image; (c) a grey-scale image of the radio structure of Cygnus A (from Perley et al. 1984), and (d) X-ray surface brightness contours of the Cygnus A cluster from *Einstein* IPC observations. The dashed line denotes the position angle of 115° between Cygnus A and the neighbouring rich cluster Abell 2319.

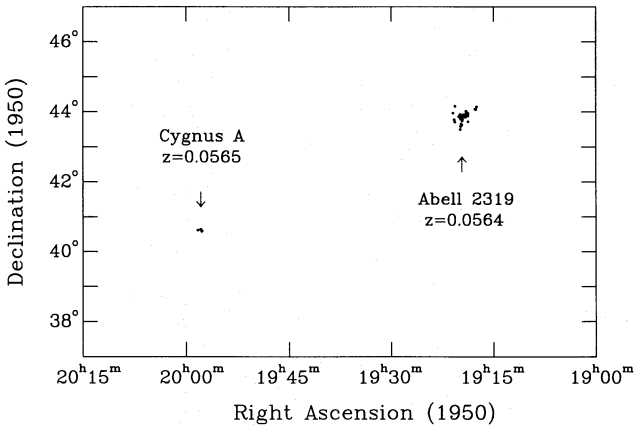

Figure 11. Cygnus A (3C 405) in relation to its surroundings. All known galaxies with measured velocities in the range 10 000–20 000 km s^{-1} have been plotted (galaxies around Cygnus A are from Spinrad & Stauffer 1982). The separation between Cygnus A and Abell 2319 is 21 h^{-1} Mpc, along a position angle of 115°.

cluster is also elongated in a similar position angle of 45°, as revealed by both optical and X-ray observations (McMillan et al. 1989; West 1989). Abell 262 forms part of the famous Persus–Pisces supercluster chain; its two nearest neighbours are Abell 347 and Abell 426, which lie $\lesssim 15\ h^{-1}$ Mpc away. As can be seen from Fig. 13, the radio axis exhibits some tendency to 'point' along the local large-scale filament towards these neighbouring clusters.

Clearly, a more systematic study of this sort of alignment effect in low-redshift BCGs is needed (a preliminary effort has been reported by Andernach et al. 1993). Nevertheless, the examples presented here suggest that BCGs with radio axes that appear to 'know' about the mass distribution of the host galaxy, as well as the surrounding distribution of neighbouring clusters, may be common.

It should be cautioned, however, that one can imagine a number of ways in which preferred radio axis orientations that may have once occurred in young BCGs at high redshifts could have been destroyed over time. For example,

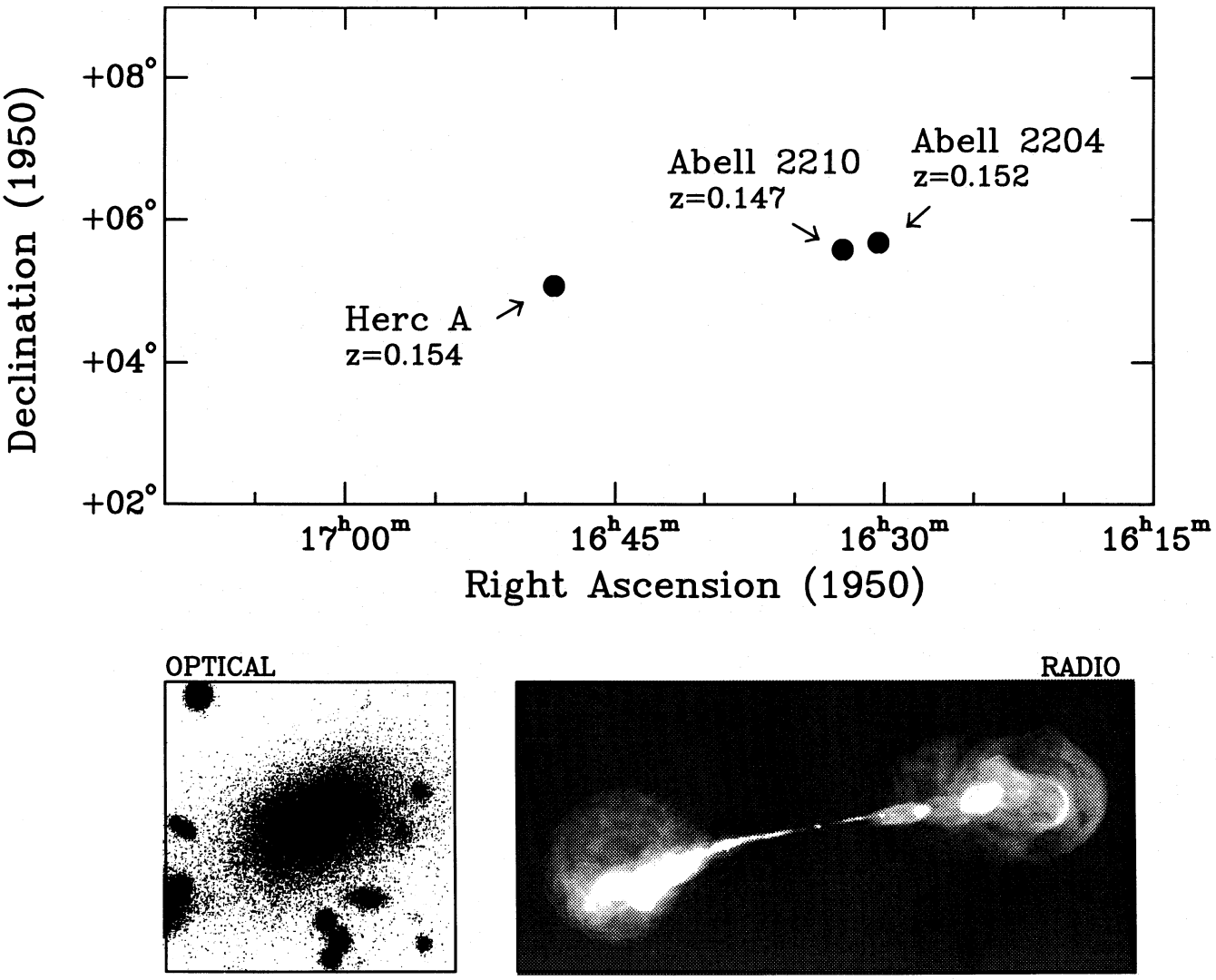

Figure 12. Hercules A (3C 348) in relation to its surroundings. The lower panels show optical and radio images of Her A (from Yates et al. 1989 and Dreher & Feigelson 1984, respectively). Note the similarity between the orientation of the optical and radio axes of Her A and the direction towards the neighbouring Abell clusters.

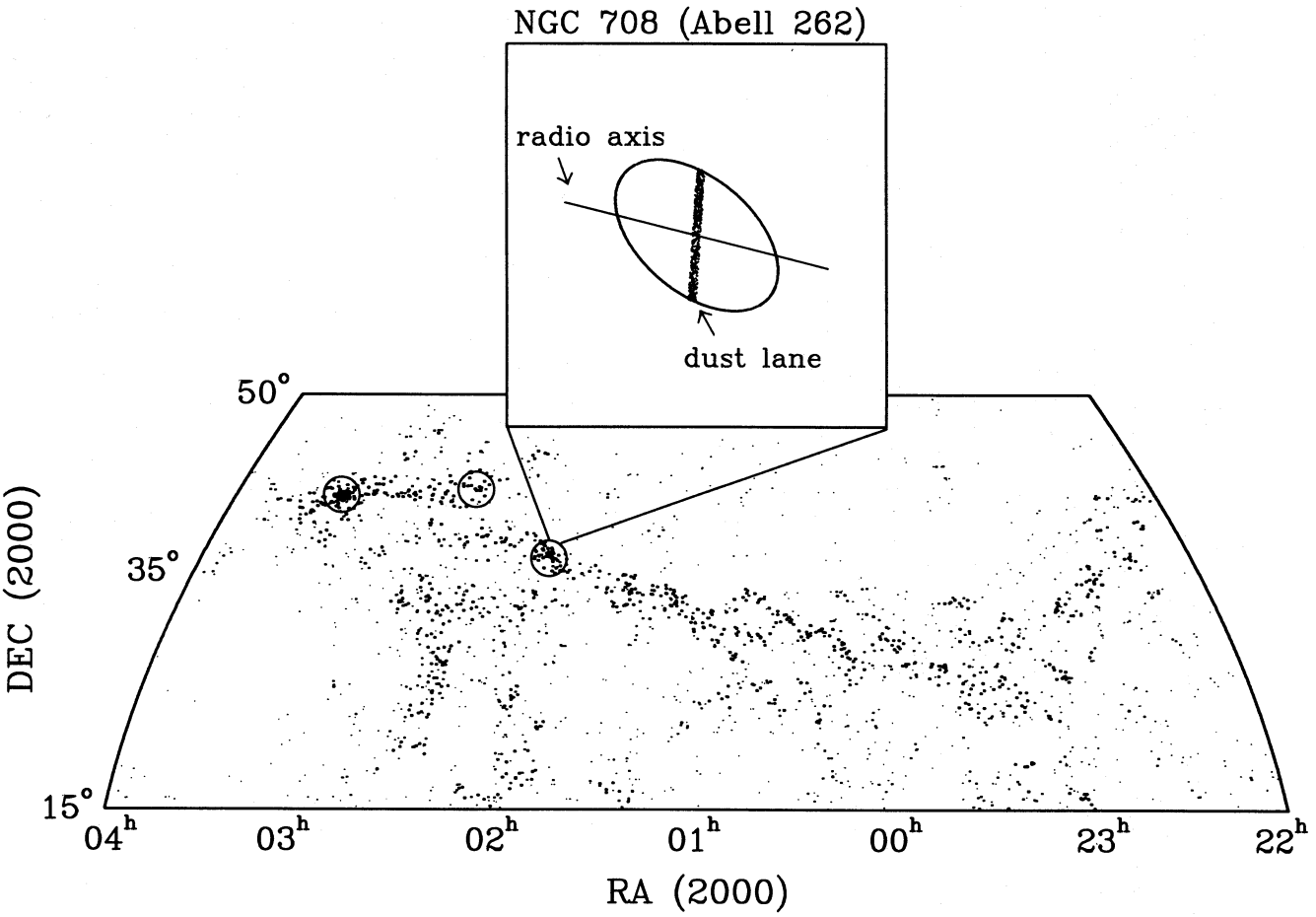

Figure 13. Comparison of the radio, optical and dust-lane orientations in NGC 708 with its large-scale environs. Plotted here is the distribution of 1395 galaxies from the RC3. Symbol sizes are proportional to local galaxy density, as in Fig. 6. Circles denote Abell clusters (in order of increasing right ascension: Abell 262, 347 and 426). The inset shows a schematic representation of the shape and orientation of NGC 708 (ellipse), its radio axis and its dust lane.

if radio sources associated with BCGs today are fuelled primarily by cooling flows rather than galaxy mergers, then the slow, quasi-spherical accretion of material might significantly alter the angular momentum of the black hole over time. A rate of only 1 $M_\odot$ yr^{-1} of cooling-flow deposition on to a black hole over a span of $\sim 10^9$ yr could completely randomize the orientation of the black hole spin axis, thus destroying any earlier alignment of the radio jets with the principal axes of the parent galaxy. Alternatively, as discussed in Section 2.5, BCGs today may be less prolate than their high-z ancestors owing to more isotropic mergers at low redshifts. Additionally, the cores of cannibalized galaxies might also survive as distinct components within BCGs (see Bender 1992 for a review), thus decoupling the gravitational potential in the innermost regions from the overall galaxy mass distribution. Hence a lack of BCG radio–optical alignments at low redshifts need not be a fatal blow to the model proposed here.

6 DISCUSSION

Although admittedly rather speculative in nature, the model proposed here is built upon a foundation of widely accepted theoretical ideas about galaxy formation and the physics of radio sources. What is novel about the present work is that it brings together for the first time a number of seemingly disparate points into a cohesive picture. The most attractive feature of this model is that it unites two alignment effects which had previously been assumed to be completely independent phenomena.

Clearly, *some* special process has caused the major axes of BCGs to be aligned with their environs on scales of many Mpc; the anisotropic merger model proposed here would seem to provide a plausible explanation for this phenomenon. If one accepts the premise that powerful radio galaxies at high redshifts are simply dynamically young BCGs, then it does not require an unreasonable leap of faith to assume that an anisotropic merger process that can produce cD galaxies with built-in preferred orientations on kpc and sub-kpc scales might also communicate these anisotropies to the very innermost regions, right down to the central engines. Indeed, given the standard accretion disc model for black hole formation and evolution (Section 4), one could argue that it would be rather surprising if the spin axes of these objects were completely divorced from their surroundings.

The basic idea of a dynamical, merger-driven origin for high-redshift radio galaxies was foreshadowed by Baade & Minkowski's (1954) suggestion that Cygnus A represents a collision between two galaxies. More recently, Djorgovski et al. (1987) and West (1991a,b) speculated that mergers might somehow influence the radio jet orientations in high-z radio galaxies, although neither study was able to offer a plausible physical mechanism that could explain the origin of such a connection. The present paper fills in that crucial gap.

Any successful model should strive not only to explain existing observations, but also to make specific predictions that can be tested. The model described here allows the following clear predictions to be made.

(i) *Anisotropic distribution of subclusters in clusters.* It is widely believed that we are currently in the epoch of rich cluster formation. If BCG and cluster alignments were the result of previous mergers which occurred along preferred axes, then one would expect that material should continue to infall anisotropically into rich clusters today. Consequently, if the formation scenario envisaged here is correct, *one expects that subclusters detected in Abell clusters will generally be distributed along the cluster and BCG major axis, as well as the direction towards other neighbouring clusters.* The growing body of observational data (both optical and X-ray) and ongoing efforts to identify substructures in Abell clusters should allow this prediction to be tested statistically in the near future.

(ii) *Dust lanes in cD glaxies.* A systematic study of the orientations of dust lanes in BCGs would provide a direct test of the hypothesis that these galaxies have prolate shapes. *Such dust lanes should show a clear tendency to align with the minor axis of the galaxy.* Unfortunately, with the exceptions of Cygnus A and NGC 708, the author is unaware of any examples of dust lanes in cD galaxies (see e.g. the compilation of Ebneter & Balick 1985). Nevertheless, it seems likely that some BCGs may have faint dust lanes that can be detected.

(iii) *ROSAT observations of high-redshift radio galaxies.* The alignment of the radio and optical axes of 3C 356 with the X-ray contours of its parent cluster (Fig. 8) should be typical of high-redshift BCGs if the anisotropic merger model is correct. The higher resolution of *ROSAT* compared to the *Einstein* satellite will allow better mapping of the distribution of hot X-ray gas in distant clusters. *It is predicted that these will show a clear correlation between the major axes of distant clusters and the radio jet orientations.*

(iv) *Companion galaxies at high redshifts.* Given the proposed anisotropic distribution of material surrounding protoBCGs, companion galaxies around high-z radio galaxies and radio-loud quasars should also be anisotropically distributed. *It is predicted that a statistical analysis of the distribution of companion galaxies around high-z radio sources will show a pronounced tendency for such objects to be found in the direction defined by the radio axis.* This means not only clumps near the radio galaxy, but also other companion galaxies at distances of several hundred kpc to a Mpc or more that are infalling anisotropically (e.g. Fig. 5). This is a particularly direct test of this model, since galaxies located far beyond the radio lobes clearly cannot be explained by jet-induced star formation or scattered light models.

(v) *Alignments of neighbouring radio galaxies at high redshifts.* If the model proposed here is correct, then *the alignments of neighbouring radio sources at high redshifts discovered by West (1991a,b) should be confirmed with larger samples.* Because one cannot really increase the number of powerful 3C-type sources, it is necessary to wait for larger quasar and radio galaxy surveys in order to identify nearby neighbours of powerful high-z radio galaxies. This alignment effect will presumably be strongest for the most powerful radio galaxies, since these are the most likely to correspond to BCGs.

7 CONCLUSIONS

A model for the formation of cD and powerful radio galaxies via highly anisotropic mergers has been presented here. It is argued that two observed alignment effects – the alignment of the radio–optical–infrared components of high-z radio galaxies, and the alignments of BCGs with their surroundings at low redshifts – are in actuality *related* phenomena that have a common origin. The basic features of this model can be summarized as follows.

(1) Powerful radio galaxies at high redshifts are the precursors of cD galaxies at low redshifts; they are simply the same objects seen at different stages in their evolution. The selection of distant galaxies on the basis of their enormous radio powers favours BCG over non-BCG galaxies.

(2) These galaxies are formed by hierarchical merging of smaller protogalactic lumps. Most importantly, *the merger process is highly anisotropic.* Driven by large-scale anisotropies in the primordial density field, these mergers tend to occur in preferred directions. This unique formation history produces galaxies that are *prolate* in shape and have preferred orientations with respect to their surroundings. Such a formation scenario can account quite naturally for the observed tendency of BCGs at low redshifts to be aligned with the major axes of their parent clusters as well as the galaxy distribution on larger scales. This is also the reason for the clumpy and elongated appearances which are characteristic of radio galaxies at high redshifts.

(3) Cold gas which falls into these galaxies during the merger process provides a plentiful source of material for the creation and nourishment of a central black hole. The *prolate* gravitational potential of these galaxies leads to the formation of a gaseous accretion disc and central black hole whose spin axes are aligned with the *major* axis of the galaxy, and hence the radio jets are also directed along the *major* axis of the galaxy. This is the origin of the radio–optical–infrared alignments seen in powerful high-z radio galaxies. The infrared and optical continua of these galaxies thus reflect the gravitational potential of the underlying stellar mass distribution. Other proposed mechanisms for the origin of the high-z alignments, such as scattering or jet-induced star formation, are likely to be only second-order effects which may enhance the alignments.

(4) Because the radio jet orientation is correlated with the structure of the underlying host galaxy, and the orientation of the latter is determined by anisotropies in the surrounding matter distribution on cluster and supercluster scales, this suggests that the radio axes of these objects reflect the developing large-scale clustering pattern in the early

Universe. Hence observational studies of the relative orientations of neighbouring radio galaxies at high redshifts can be used as a proxy to search for evidence of BCG alignments at high redshifts, thus providing a unique probe of the cosmological density field at early epochs.

In conclusion, the model presented here suggests the existence of a truly remarkable coherence of structures over many orders of magnitude, from the central engines of powerful radio galaxies to the very large-scale structure of the Universe.

ACKNOWLEDGMENTS

I am grateful to a number of friends and colleagues for generously providing me with observational data, simulations and helpful comments. In particular, I wish to thank Jim Schombert for sending me his CCD images of NGC 4889 and Cygnus A, Ray Carlberg for making his *N*-body simulation available to me, and John Dreher for sending me the VLA image of Hercules A. I also thank John Peacock, Paddy Leahy and Carolin Crawford for permission to reproduce their published data here. Last, but not least, it is a pleasure to thank Ray Carlberg, Neal Jackson, George Miley, John Peacock, Sidney van den Bergh and the referee, James Dunlop, for enlightening discussions and comments which helped to improve this paper. This work was supported by the Netherlands Foundation for Research in Astronomy (ASTRON).

REFERENCES

Andernach H., West M. J., Kotanyi C., Unewisse A. M., 1993, in Chincarini G., Iovino A., Maccacaro T., Maccagni D., eds, ASP Conf. Ser. 51, Observational Cosmology. Astron. Soc. Pac., San Francisco, p. 123
Antonucci R., 1983, ARA&A, 31, 473
Argyres P. C., Groth E. J., Peebles P. J. E., Struble M. F., 1986, AJ, 91, 471
Arnaud K. A., Fabian A. C., Eales S. A., Jones C., Forman W., 1984, MNRAS, 211, 981
Baade W., Minkowski R., 1954, ApJ, 119, 206
Bahcall N. A., Chokshi A., 1991, ApJ, 380, L9
Bahcall N. A., Chokshi A., 1992, ApJ, 385, L33
Bahcall N. A., Soneira R. M., 1983, ApJ, 270, 20
Balick B., Heckman T. M., 1982, ARA&A, 20, 431
Bardeen J. M., Petterson J. A., 1975, ApJ, 195, L65
Bardeen J. M., Bond J. R., Kaiser N., Szalay A. S., 1986, ApJ, 304, 15
Baum S. A., Heckman T., Bridle A., van Breugel W., Miley G., 1988, ApJS, 68, 643
Beers T. C., Geller M. J., 1983, ApJ, 274, 491
Begelman M. C., Blandford R. D., Rees M. J., 1980, Nat, 287, 307
Begelman M. C., Blandford R. D., Rees M. J., 1984, Rev. Mod. Phys., 56, 255
Bender R., 1992, in Longo G., Capaccioli M., Busarello G., eds, Morphological and Physical Classification of Galaxies. Kluwer, Dordrecht, p. 357
Bertola F., 1992, in Longo G., Capaccioli M., Busarello G., eds, Morphological and Physical Classification of Galaxies. Kluwer, Dordrecht, p. 115
Bertola F., Galletta G., 1978, ApJ, 226, L115
Bhavsar S. P., 1989, ApJ, 338, 718
Bhavsar S. P., Ling E. N., 1988, ApJ, 331, L63
Binggeli B., 1982, A&A, 107, 338
Binney J. J., 1978, MNRAS, 183, 779
Blandford R. D., 1990, in Active Galactic Nuclei (Saas-Fee). Springer-Verlag, Berlin, p. 161
Blandford R. D., Rees M. J., 1974, MNRAS, 169, 395
Blumenthal G. R., Faber S. M., Primack J. R., Rees M. J., 1984, Nat, 311, 517
Bond J. R., 1986, in Madore B. F., Tully R. B., eds, Galaxy Distances and Deviations from Universal Expansion. Reidel, Dordrecht, p. 255
Bond J. R., 1987, in Faber S., ed., Nearly Normal Galaxies. Springer-Verlag, Berlin, p. 389
Bond J. R., Efstathiou G., 1984, ApJ, 285, L45
Bothun G. D., Geller M. J., Kurtz M. J., Huchra J. P., Schild R. E., 1992, ApJ, 395, 347
Buote D. A., Canizares C. R., 1992, ApJ, 400, 385
Carilli C. L., Perley R. A., Dreher J. W., Leahy J. P., 1991, ApJ, 383, 554
Carlberg R. G., 1990, ApJ, 350, 505
Carlberg R. G., 1994, ApJ, submitted
Carlberg R. G., Couchman H. M. P., 1988, ApJ, 340, 47
Carter D., Metcalfe N., 1980, MNRAS, 191, 325
Carter D., Inglis I., Ellis R. S., Efstathiou G., Godwin J., 1985, MNRAS, 212, 471
Chambers K. C., Miley G. K., 1990, in Kron R. G., ed., ASP Conf. Ser. 10, Evolution of the Universe of Galaxies. Astron. Soc. Pac., San Francisco, p. 373
Chambers K. C., Miley G. K., van Breugel W., 1987, Nat, 329, 604
Chambers K. C., Miley G. K., Joyce R. R., 1988, ApJ, 329, L75
Christodoulou C. M., Tohline J. E., 1993, ApJ, 403, 110
Crawford C. S., Fabian A. C., 1993, MNRAS, 260, L15
Daly R. A., 1990, ApJ, 355, 416
Daly R. A., 1992, ApJ, 399, 426
Davies R. L., Efstathiou G., Fall S. M., Illingworth G., Schechter P. L., 1983, ApJ, 266, 41
Davis M., Efstathiou G., Frenk C. S., White S. D. M., 1985, ApJ, 292, 371
Dekel A., Silk J., 1986, ApJ, 303, 39
de Lapparent V., Geller M. J., Huchra J. P., 1986, ApJ, 202, L1
de Serego Alighieri S., Fosbury R. A. E., Quinn P. J., Tadhunter C. N., 1989, Nat, 341, 307
de Vaucouleurs G., de Vaucouleurs A., Corwin H. G., Buta R. J., Paturel G., Fouqué P., 1991, Third Reference Catalog of Bright Galaxies (RC3). Springer-Verlag, New York
De Young D. S., 1989, ApJ, 342, L59
de Zeeuw T., Franx M., 1991, ARA&A, 29, 239
Djorgovski S., 1987, in Thuan T. X., Montmerle T., Van J. Tran Thanh, eds, Starbursts and Galaxy Evolution. Editions Frontières, Gif-sur-Yvette, p. 401
Djorgovski S., Spinrad H., Pedelty J., Rudnick L., Stockton A., 1987, AJ, 93, 1307
Djorgovski S., Weir N., Matthews K., Graham J. R., 1991, ApJ, 372, L67
Doroshkevich A. G., 1970, Astrophysica, 6, 320
Dreher J. W., 1981, AJ, 86, 833
Dreher J. W., Feigelson E. D., 1984, Nat, 308, 43
Dressler A., 1984, ARA&A, 22, 185
Dunlop J. S., Peacock J. A., 1990, MNRAS, 247, 19
Dunlop J. S., Peacock J. A., 1993, MNRAS, 263, 936
Eales S. A., 1992, ApJ, 397, 49
Eales S. A., Rawlings S., 1990, MNRAS, 243, 1P
Ebneter K., Balick B., 1985, AJ, 90, 183
Edge A. C., Stewart G. C., Fabian A. C., Arnaud K. A., 1990, MNRAS, 245, 559
Efstathiou G., Rees M. J., 1988, MNRAS, 230, 5P
Efstathiou G., Frenk C. S., White S. D. M., Davis M., 1988, MNRAS, 235, 715
Einasto J., Gramann M., Saar E., Tago E., 1993, MNRAS, 260, 705
Eisenhardt P., Chokshi A., 1990, ApJ, 351, L9
Faber S. M., 1982, in Bruck H. A., Coyne G. V., Longair M. S., eds, Astrophysical Cosmology, Ponti. Acad. Sci., Vatican City, p. 191

Fabian A. C., 1989, MNRAS, 238, 41P
Fasano G., Vio R., 1991, MNRAS, 249, 629
Fitchett M., Webster R. L., 1987, ApJ, 317, 653
Frenk C. S., White S. D. M., Davis M., Efstathiou G., 1988, ApJ, 327, 507
Geller M. J., Huchra J. H., 1989, Science, 246, 897
Gregory S. A., Thompson L. A., 1978, ApJ, 222, 784
Gunn J. E., 1979, in Hazard C., Mitton S., eds, Active Galactic Nuclei. Cambridge Univ. Press, Cambridge, p. 213
Habe A., Ikeuchi S., 1985, ApJ, 289, 540
Haehnelt M. G., Rees M. J., 1993, MNRAS, 263, 168
Hammer F., Le Fèvre O., 1990, ApJ, 357, 38
Hargrave P. J., Ryle M., 1974, MNRAS, 166, 305
Harris W. E., 1991, ARA&A, 29, 543
Hawarden T. G., Elson R. A., Longmore A. J., Tritton S. B., Corwin H. G., 1981, MNRAS, 196, 747
Haynes M. P., Giovanelli R., 1986, ApJ, 306, L55
Heckman T. M., Smith E. P., Baum S. A., van Breugel W. J. M., Miley G. K., Illingworth G. D., Bothun G. D., Balick B., 1986, ApJ, 311, 526
Hill G. J., Lilly S. J., 1991, ApJ, 367, 1
Hoessel J. G., 1980, ApJ, 241, 493
Hoessel J. G., Schneider D. P., 1985, AJ, 90, 1648
Hutchings J. B., Crampton D., Campbell B., 1984, ApJ, 280, 41
Jackson N., Sparks W. B., Miley G. K., Macchetto F., 1994, A&A, in press
Jaffe W., Ford H., Ferraresse L., van den Bosch F., O'Connell R., 1993, Nat, 364, 213
Jorgensen I., Franx M., Kjaergaard P., 1992, A&AS, 95, 489
Kahn F., Woltjer L., 1959, ApJ, 130, 705
Kaiser N., 1984, ApJ, 284, L9
Kofman L., Pogosyan D., Shandarin S. F., Melott A. L., 1992, ApJ, 393, 437
Kotanyi C., Ekers R. D., 1979, A&A, 73, L1
Lambas D. G., Groth E. J., Peebles P. J. E., 1988, AJ, 95, 996
Lambas D. G., Nicotra M., Muriel H., Ruiz L., 1990, AJ, 100, 1006
Lauer T. R., 1988, ApJ, 325, 49
Leahy J. P., Muxlow T. W. B., Stephens P. W., 1989, MNRAS, 239, 401
Le Fèvre O., Hammer F., 1988, ApJ, 333, L37
Le Fèvre O., Hammer F., Jones J., 1988, ApJ, 331, L73
Leir A. A., van den Bergh S., 1977, ApJS, 34, 381
Lilly S. J., 1990, in Kron R. G., ed., ASP Conf. Ser. 10, Evolution of the Universe of Galaxies. Astron. Soc. Pac., San Francisco, p. 345
Lilly S. J., Longair M. S., 1984, MNRAS, 211, 833
Little B., Weinberg D. H., Park C., 1991, MNRAS, 253, 295
Lynden-Bell D., 1969, Nat, 223, 690
McCarthy P. J., 1993, ARA&A, 31, 639
McCarthy P. J., van Breugel W., 1989, in Frank C. et al., eds, The Epoch of Galaxy Formation. Kluwer, Dordrecht, p. 57
McCarthy P. J., van Breugel W. J., Spinrad H., Djorgovski S., 1987, ApJ, 321, L29
McMillan S. L. W., Kowalski M. P., Ulmer M. P., 1989, ApJS, 70, 723
Matthews T. A., Morgan W. W., Schmidt M., 1964, ApJ, 140, 35
Mazure A., Proust D., Mathez G., Mellier Y., 1988, A&AS, 76, 339
Mellier Y., Mathez G., Mazure A., Chauvineau B., Proust D., 1988, A&A, 199, 67
Melott A. L., Shandarin S. F., 1989, ApJ, 343, 26
Merritt D., 1985, ApJ, 289, 18
Merritt D., de Zeeuw T., 1983, ApJ, 267, L19
Miley G. K., 1992, in Benvenuti P., Schreier E., eds, ECF/STScI Conf. and Workshop Proc. No. 44, Science with the Hubble Space Telescope. European Southern Observatory, Munich, p. 1
Miley G. K., Chambers K. C., van Breugel W. J. M., Macchetto F., 1992, ApJ, 401, L69
Nusser A., Dekel A., 1990, ApJ, 362, 14
Oegerle W. R., Hoessel J. G., 1991, ApJ, 375, 15
Owen F. N., Laing R. A., 1989, MNRAS, 238, 357
Parma P., de Ruiter H. R., Fanti C., Fanti R., 1986, A&AS, 64, 135
Peacock J. A., 1991, MNRAS, 253, 1P
Peacock J. A., Heavens A. F., 1985, MNRAS, 217, 805
Peacock J. A., West M. J., 1992, MNRAS, 259, 494
Peebles P. J. E., Dicke R. H., 1968, ApJ, 154, 891
Perley R. A., Dreher J. W., Cowan J. J., 1984, ApJ, 285, L35
Plionis M., Valdarnini R., Jing Y. P., 1992, ApJ, 398, 12
Porter A. C., Schneider D. P., Hoessel J. G., 1991, AJ, 101, 1561
Press W. H., Schechter P., 1974, ApJ, 187, 425
Rees M. J., 1978, Nat, 275, 516
Rees M. J., 1989, MNRAS, 239, 1P
Rhee G., Katgert P., 1987, A&A, 183, 217
Rhee G., van Haarlem M., Katgert P., 1992, AJ, 103, 1721
Rigler M. A., Lilly S. J., Stockton A., Hammer F., Le Fèvre O., 1992, ApJ, 385, 61
Rocca-Volmerange B., Guiderdoni B., 1990, MNRAS, 247, 166
Rood H. J., Sastry G. N., 1971, PASP, 80, 313
Ryden B. S., Lauer T. R., Postman M., 1993, ApJ, 410, 515
Sadun A. C., Hayes J. J. E., 1993, PASP, 105, 379
Salpeter E. E., 1964, ApJ, 140, 796
Sandage A., 1976, ApJ, 205, 6
Sastry G. N., 1968, PASP, 80, 252
Schombert J. M., 1988, ApJS, 64, 643
Schombert J. M., 1992, in Longo G., Cappacioli M., Busarello G., eds, Morphological and Physical Classification of Galaxies. Kluwer, Dordrecht, p. 53
Schwartz D. A., Bradt H. V., Remillard R. A., Tuohy I. R., 1991, ApJ, 376, 424
Simkin S. M., 1977, ApJ, 217, 45
Small T. A., Blandford R. D., 1992, MNRAS, 259, 725
Soltan A., 1982, MNRAS, 200, 115
Spinrad H., 1989, in Frenk C. S. et al., eds, The Epoch of Galaxy Formation. Kluwer, Dordrecht, p. 39
Spinrad H., Stauffer J. R., 1982, MNRAS, 200, 153
Steiman-Cameron T. Y., Durisen R. H., 1988, ApJ, 325, 26
Stockton A., 1993, in Rocca-Volmerange B., Guiderdoni B., Dennefeld H., Tran Thanh Van J., eds, First Light in the Universe: Stars or QSOs? Editions Frontières, Gif-sur-Yvette, p. 239
Struble M. F., 1990, AJ, 99, 743
Struble M. F., Peebles P. J. E., 1985, AJ, 90, 582
Struble M. F., Rood M. J., 1987, ApJS, 63, 555
Struble M. F., Rood H. J., 1991, ApJS, 77, 363
Tohline J. E., Simonson G. F., Caldwell N., 1982, ApJ, 252, 92
Toomre A., 1977, in Tinsley B., Larson R., eds, The Evolution of Galaxies and Stellar Populations. Yale Univ. Obs., New Haven, p. 401
Tremaine S., 1990, in Wielen R., ed., Dynamics and Interactions of Galaxies. Springer-Verlag, Berlin, p. 394
Tremaine S., Richstone D. O., 1977, ApJ, 212, 311
Trevese D., Cirimele G., Flin P., 1992, AJ, 104, 935
Tubbs A. D., 1980, ApJ, 241, 969
Turner E. L., 1991, AJ, 101, 5
van Albada T. S., Kotanyi C. G., Schwarzschild M., 1982, MNRAS, 198, 303
van Breugel W., Fillipenko A. V., Heckman T., Miley G. K., 1985, ApJ, 293, 83
van den Bergh S., 1976, ApJ, 210, L63
van den Bergh S., 1983, PASP, 95, 275
van Kempen E., Rhee G. F. R. N., 1990, A&A, 237, 283
Vestergaard M., Barthel P. D., 1993, AJ, 105, 456
Villumsen J. V., 1982, MNRAS, 199, 493
Villumsen J. V., 1983, MNRAS, 204, 219
Vogeley M. S., Park C., Geller M. J., Huchra J. P., 1992, ApJ, 391, L5
Warren M. S., Quinn P. J., Salmon J. K., Zurek W. W., 1992, ApJ, 399, 405
Weinberg D. H., Gunn J. E., 1990, MNRAS, 247, 260

West M. J., 1989, ApJ, 347, 610
West M. J., 1991a, ApJ, 379, 19
West M. J., 1991b, in Crampton D., ed., ASP Conf. Ser. 21, The Space Distribution of Quasars. Astron. Soc. Pac., San Francisco, p. 290
West M. J., 1993a, in Rocca-Volmerange B., Guiderdoni B., Dennefeld M., Tran Thanh Van, J., eds, First Light in the Universe: Stars or QSOs? Editions Frontières, Gif-sur-Yvette, p. 425
West M. J., 1993b, MNRAS, 265, 755
West M. J., 1994, PASP, in press
West M. J., Dekel A., Oemler A., 1989, ApJ, 336, 46
West M. J., Villumsen J. V., Dekel A., 1991, ApJ, 369, 287
White S. D. M., 1978, MNRAS, 184, 185
White S. D. M., 1979, MNRAS, 189, 831
White S. D. M., Frenk C. S., 1991, ApJ, 379, 52
White S. D. M., Frenk C. S., Davis M., Efstathiou G., 1987, ApJ, 313, 505
White S. D. M., Briel U. G., Henry J. P., 1993, MNRAS, 261, L8
Wirth A., Smarr L., Gallagher J. S., 1982, AJ, 87, 602
Yates M. G., Miller L., Peacock J. A., 1989, MNRAS, 240, 129
Yee H. K. C., Green R. F., 1987, ApJ, 319, 28
Zeldovich Ya. B., 1970, A&A, 5, 84